

# In pursuit of highly accurate atomic lifetime measurements of multiply charged ions

E Träbert

Astronomisches Institut, Fakultät für Physik und Astronomie, Ruhr-Universität Bochum,  
D-44780 Bochum, Germany

and

Physics Division, Lawrence Livermore National Laboratory, Livermore, CA 94550, USA

E-mail: [traebert@astro.rub.de](mailto:traebert@astro.rub.de)

Received 6 June 2009, in final form 2 September 2009

Published 19 March 2010

Online at [stacks.iop.org/JPhysB/43/074034](http://stacks.iop.org/JPhysB/43/074034)

## Abstract

Accurate atomic lifetime data are useful for terrestrial and astrophysical plasma diagnostics. At accuracies higher than those required for these applications, lifetime measurements test atomic structure theory in ways complementary to spectroscopic energy determinations. At the highest level of accuracy, the question arises whether such tests reach the limits of modern theory, a combination of quantum mechanics and QED, and possibly point to physics beyond the standard model. If high-precision atomic lifetime measurements, especially on multiply charged ions, have not quite reached this high accuracy yet, then what is necessary to attain this goal?

(Some figures in this article are in colour only in the electronic version)

## 1. Introduction

'25–30% accuracy in atomic rates is often inadequate for high-resolution x-ray observations from existing satellites' [1]. This statement by a representative of one of the leading astrophysics institutes (Harvard–Smithsonian Centre for Astrophysics) is certainly correct. There are many astrophysics problems in which atomic transition rates are not known well enough. In many other cases, the actual rates are of minor importance. However, the balance of collisional excitation and radiative decay rates matters for the level populations which result in line (intensity) ratios which in turn are exploited to derive information on plasma density and temperature. However, are radiative transition rates that poorly known? Certainly not all of them: in the last four decades, beam–foil spectroscopy has produced many hundred atomic level lifetimes (the inverse of the sum of all decay rates of a given level) with accuracies (in most cases) in the range of 10–5%, with occasional 1% measurements under favourable circumstances. Laser measurements of fast atom and (singly charged) ion beams have yielded many lifetimes and transition rates with similar accuracies, and some of them

with uncertainties as small as about 0.1%, in agreement with some novel molecular techniques. Over the last about 15 years, ion trap measurements of more than 60 spin-forbidden and electric-dipole-forbidden transitions have reached accuracies between 3 and 0.3% (some claims go even farther)—also on various x-ray transitions of astrophysical interest. These achievements do not invalidate the above statement, but they show that it does not reflect the state of the art.

In the following, I will briefly discuss precision lifetime experiments as have been pursued in the last, say, three decades using ion beam and laser techniques (or combinations thereof), mostly aiming at electric dipole transitions. These experiments have revealed various systematic error problems. Some of these seemed irrelevant when precision studies of the much longer lifetimes of levels decaying by spin-forbidden or E1-forbidden transitions began about a decade ago, utilizing ion traps of various designs. However, some of the earlier problems have recurred even as the lifetimes in question exceed the previously studied ones by some eight orders of magnitude. I will then describe in some detail various recent experiments that aim at 'quality' atomic lifetime data (accurate to better than, say, 3%) for understanding terrestrial and astrophysical

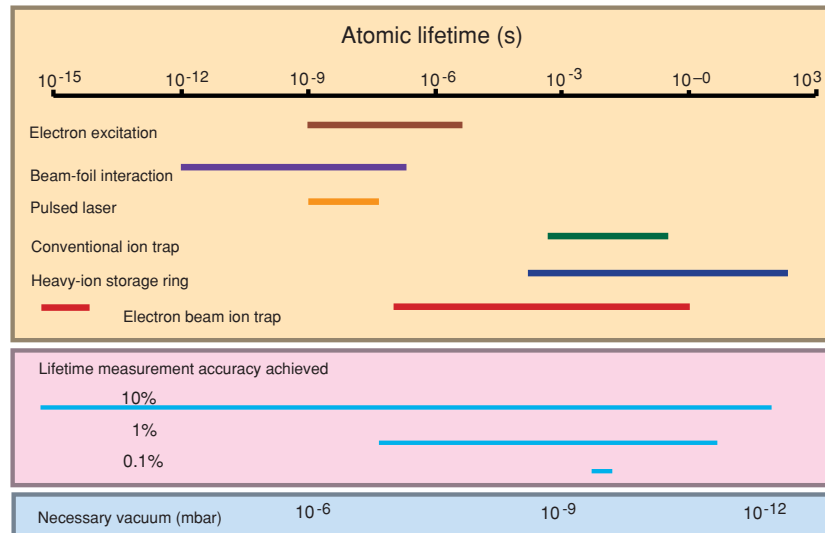


**Figure 1.** Atomic lifetime measurement ranges covered by various techniques and the typical vacuum in the apparatus. For the measurement of long lifetimes, excellent vacuum is essential, but not sufficient: the low signal rate competes with the detector noise. The optimum lifetime range for high accuracy work seems to lie near 10 ms. Because of photocathode materials, there is also an optimum spectral range for ‘optical’ observations in the far-UV and VUV (solar blind detectors), and in the x-ray range.

plasmas, or aim at extreme accuracy (better than 0.5%) in the pursuit of testing atomic structure theory in the combination of quantum mechanics and QED. In order to reach significant accuracy, the experiments have to cope with a number of sources of systematic error, some of which offer insight into interesting phenomena.

Atomic lifetimes can be interpreted as the damping of a classical oscillator, and therefore they can be measured either as the width of a damping curve or as the time constant of an exponential decay. Mathematically, the Fourier transform of an exponential is a Lorentzian. Measuring the width of the Lorentzian (in practice, of the Lorentzian part of a Voigt profile in which the Gaussian contribution from collisions—a density effect—may furthermore be affected by instrumental effects) is equivalent to determining the time constant of an exponential decay curve (in practice complicated by detector noise and many other problems). The determination of the position of a spectral line (assumed to be fairly symmetric) usually requires only a few measurement points (and a fit of a line profile to the data) and a relatively crude reference to an accurately known standard to benefit from the knowledge of that standard; high accuracy results from the many diverse efforts that have contributed to establishing the standard. In contrast, measuring decay curves is intrinsically less accurate, because the benefit of symmetry of the data distribution is unavailable—a curve *shape* has to be determined with accuracy; moreover, any fit procedures involving exponential decays are nonlinear. As a result, lifetime measurements carry all the uncertainty of the practical experiment, from data statistics and detector dark rate to systematic error. Hence, lifetime measurements with uncertainties of, say, 0.1% are considered highly accurate, whereas wavelength measurements to the same accuracy would be judged as being rather crude, since interferometry and laser techniques have produced so many wavelengths of uncertainties in the  $10^{-6}$  range, and the leading edge in the atomic structure and atomic

clock research aims at the  $10^{-18}$  range. And yet, accurate lifetime measurements probe atomic structure details that the other techniques do not.

Figure 1 gives an overview of the lifetime measurement ranges discussed in this paper. Figure 2 sketches some of the basic lifetime measurement geometries that will be discussed in the following sections. The paper reports on experimental studies of electric-dipole-allowed (section 2) and of electric-dipole-forbidden transitions (section 3) separately, because the typical atomic lifetime ranges for the two classes tend to differ very much for the ionization stages that are of particular interest and that are experimentally accessible.

## 2. Electric dipole decays

Electric dipole (E1) decays are the most common species, the leading term of the multipole expansion of the radiation field. In neutral atoms and low-charge ions, the associated excitation levels have lifetimes on the order of nanoseconds to picoseconds.  $\Delta n \neq 0$  transitions between levels of different principal quantum numbers  $n$  are considered to be largely hydrogenic and thus the level lifetimes are easily calculated (if one neglects configuration mixing, etc in multi-electron systems). The level lifetimes scale as  $Z^{-4}$  and vary therefore rather steeply along the isoelectronic sequence. (The useful concept of isoelectronic sequences was promoted by series expansions of atomic parameters, including oscillator strengths, line strengths, and transition rates or  $A$  values, some 80 years ago by Hylleraas.) Isoelectronic trends of highly accurate lifetime data would be very valuable to establish, but—given the rarity of highly precise lifetime measurements—most such (rare) data are singular in their isoelectronic sequence so far. Readers interested in those isoelectronic systematics may want to look up presentations in various textbooks, on the web [2], or in classical papers on the subject [3, 4].)

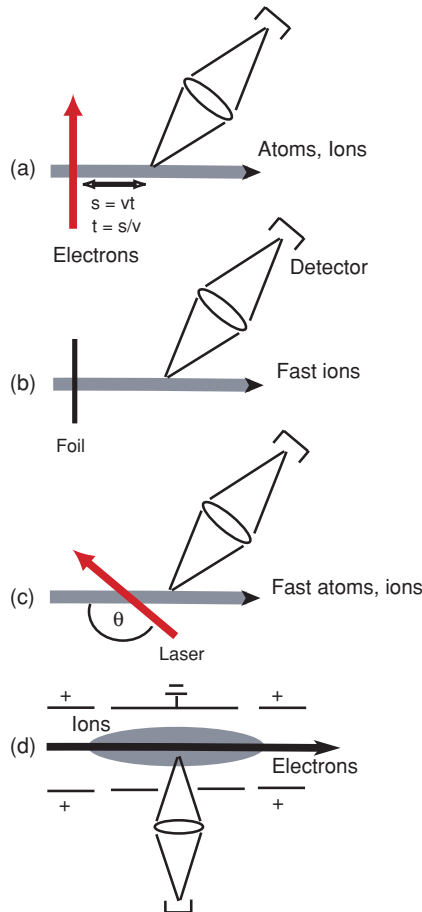


**Figure 2.** Atomic lifetime measurement techniques for short and long lifetimes. For short lifetimes (pico- through nanoseconds), a beam of atoms or ions is being excited (a) by electron collisions, (b) by being passed through a material target or (c) by interaction with laser light. If the particle velocity is high enough, the spatial separation of the excitation and observation zones can be exploited as a measure of time after excitation. For long lifetimes (microseconds to seconds), a stationary ion cloud (d) is kept trapped by the electric fields between cylindrical drift tubes; the ions in the trap may be excited by a dense electron beam (especially so in the electron beam ion trap), while the time measurement uses electronic timing.

In contrast to hydrogen-like (one electron overall) and hydrogenic (one highly excited valence electron) ions, atomic systems with several electrons may also have several electrons in the valence shell, and the (E1 decay dominated) lifetimes of these levels scale much less steeply with the ion charge  $\zeta$  or the nuclear charge  $Z$ , for example (in most cases), as  $Z^{-1}$ . Such transitions can be measured over a wide range of nuclear charges. Transitions that require a spin change (intercombination transitions) or higher multipole order radiation scale more steeply with high powers of  $Z$ , but they begin (at low  $Z$ ) with very low rates. Typically each type of transition has a window of measurement opportunity somewhere along the respective isoelectronic sequence. The much longer lifetimes of levels with only E1-forbidden decays (milliseconds to seconds) will be discussed in the section on ion traps.

The wavelengths of the transitions vary with  $Z$ , too, and optimal detectors for certain wavelength ranges determine a second window of opportunity. For highly accurate lifetime measurements, both windows have to coincide on the same ion.

### 2.1. Early days

At the beginning of the 20th century, studies of atomic spectra under the influence of strong electric fields suffered from the problem of breakdown of the high voltage due to charge carriers in the low-pressure discharge between the electrodes which were mounted in a vacuum vessel—high vacuum technology was only just emerging. In one of the pioneering experiments Stark reduced the problem by shooting canal rays (ions inside the vacuum of a cathode ray tube, travelling in a direction opposite to Thomson's (electron) cathode rays) across the space between the high-voltage electrodes. The observed Stark effect bears witness to his success. In the 1920s the idea was revived by Wien [5] who recognized that the ions in cathode rays were travelling fast enough so that photographic images of the light emission along the canal ray track might reveal the time after excitation that the ions needed to re-emit the excitation energy. The concept was valid, but various technical aspects precluded any meaningful atomic lifetime measurement at the time. With lifetime estimates in the nanosecond range,  $\alpha$  particles of 1 MeV energy (available only from radioactive sources, before the advent of ion accelerators) travel some 7 mm in a nanosecond, and heavier ions even less. Such a decay path inside a glass apparatus would have to be observed by photography using none-too-efficient photographic plates of nonlinear response to light. The residual gas in the cathode ray tube would be excited collisionally by whatever fast particles, and this nonuniform background glow would be superimposed on any (rather weak) decay signal.

More than three decades later, experimenters returned to the same technique. By that time, heavy-ion accelerators delivered multi-MeV ion beams of many elemental species (for nuclear physics), in vacuum systems that with diffusion pumps typically reached  $10^{-5}$  mbar of pressure, which ensured ion path lengths of some 30–100 m between collisions with the residual gas atoms. Better photographic plates had been produced—but nobody seemed to remember Wien's experiments. The 1920s had been an active period for atomic physics, but after world war II, the fashion had turned to nuclear physics. For detecting the products of nuclear reactions, physicists had x-ray (keV energy photon) and particle (MeV energy) detectors, but no mental link to anything in the range of visible light (eV range). They had windows in their metal vacuum chambers only to control the mechanical set-ups inside. There is anecdotal evidence of several people who saw light emission near their thin-foil nuclear targets under ion beam irradiation. Apparently only two nuclear physicists (Kay and Bashkin [6–9]) realized that they saw atomic physics at work and how this could be exploited with substantial scientific profit, including the determination of atomic lifetimes (see the next subsection).

Atomic physicists meanwhile had chosen a different path, bombarding an atomic beam with a pulsed electron beam (figure 2(a)) and registering the delayed emission. In these time-resolved measurements, photoelectric detectors replaced photographic emulsions. Data acquisition electronics was based on vacuum tubes, and the nanosecond lifetimes which are typical of electric dipole decays of neutral atoms were at the limit of measurement capability, far from enabling notable accuracy. Not only the detection, the provision of pulsed electron beams also required vacuum tubes and thus suffered from their frequency limitations, too. Photomultipliers at the time were too noisy for single photon detection; experiments therefore evaluated the phase shift between pulse trains of excitation and of a detected photocurrent signal in order to determine the time delay between the two.

Many of the limitations imposed by the technical problems have since been overcome (that is, shifted by a few orders of magnitude). However, even with the older technology, some lasting insight was gained that pertains to the most recent high-accuracy lifetime measurements. In any photon-starved experiment, one would like to maximize the signal, perhaps (in this case) by increasing the beam current of the exciting electron beam. It is easier to obtain a higher current electron beam, if the beam energy is increased. Bennett and Kindlmann [10] showed that the decay curves obtained at electron beam energies just above excitation threshold and well above that threshold differ qualitatively, because higher levels of the target atoms may be excited as well and in their decay repopulate the level of interest. The decay curves then feature significantly different slopes depending on the contribution of cascades. This effect can lead to a severe misinterpretation of the lifetime results extracted. Bennett and Kindlmann quote uncertainties of 1–3% for their  $2p^53p$  level lifetime measurements in Ne atoms when avoiding this significant systematic error. I take this error range as a threshold defining ‘precision lifetime measurements’ for part of the following discussion, and uncertainties of 0.5% and less as a qualifier for high-accuracy measurements. The distortions of decay curves by radiative cascades such as recognized by Bennett and Kindlmann, and the quest for selective excitation as a means to avoid cascades, have become recurrent themes throughout the subsequent developments.

## 2.2. Straight fast ion beams

There are hundreds of reports and numerous reviews on atomic lifetime measurements using fast ion beams, mostly exciting the ions by sending the beams through thin carbon foils (hence ‘beam-foil spectroscopy’, see figure 2(b)). Some of the more recent ones [11–13] with their many references may be most suitable as entry points for a reader interested in more detail than is appropriate here.

Fast ion beams for atomic physics typically range in energy from some 10 keV (for light ions) to some GeV (for selected heavy ions). Such a wide range cannot be produced by one given accelerator, but only by a range of types of accelerators, for the higher ion energies often incorporating several accelerator stages that operate on different techniques.

The higher the desired ion energy, the larger the machine and the cost of building it, and the fewer the machines in each class. The ion beam velocity varies (roughly) as the square root of the beam energy;  $^4\text{He}$  atoms or ions at 10 keV travel  $0.7\text{ mm ns}^{-1}$  (0.23% of the speed of light), whereas  $^{238}\text{U}$  nuclei at about  $420\text{ MeV amu}^{-1}$  (100 TeV total) travel 0.22 m in the same nanosecond ( $\beta = v/c \approx 0.72$ ). (The latter example describes uranium ions fast enough to lose all 92 electrons in passage through a solid material.) A practical number of  $0.5\text{ MeV amu}^{-1}$  is provided for ion beams as they travel at a velocity near to  $10\text{ mm ns}^{-1}$ . Since all ions in a beam travel at about the same velocity, time of flight corresponds to distance, and in many cases a distance measurement of sufficient precision requires only a moderate mechanical effort, but can replace a time measurement that in the nanosecond or picosecond time range would be demanding, if not impossible, to do with similar precision. In the last example, a ruler with 1 cm tick marks corresponds to a 1 ns clock interval, and mechanical displacements by  $10\text{ }\mu\text{m}$ —an easy feat—correspond to 1 ps.

The velocity of an ion beam is usually measured by the acceleration voltage used in electrostatic machines, or by the momentum selection offered in the deflection when passing an ion beam through a magnetic field. For ion beams of moderate energy (say, less than 100 keV), a curved cylindrical capacitor (an electric sector field) can be employed to deflect the ion beam and thus measure the ion energy. For high-energy ion beams with a pulse structure (from radiofrequency acceleration stages or cyclical acceleration devices), pick-up coils at a well-measured distance can detect the time of flight interval needed to cover the distance between the coils and thus determine the ion velocity. All of these techniques are inherently limited to a practical uncertainty no better than some  $10^{-3}$ , and only under exceptional care has the  $10^{-4}$  mark been approached.

The velocity at observation is not necessarily the same as at production. In most cases, especially for highly charged ions, the desired ion charge state is reached only after one or more steps of ion-matter interaction, and so is excitation. Any collision between the beam particles and a gaseous or solid, or even an electron target, changes the velocity vector. Distant collisions (large collision parameter, and thus a large cross section by virtue of geometry) go along with small momentum transfer, and the beam ions experience only small-angle scattering and a relatively small energy loss (‘electronic energy loss’), whereas in collisions with the (small) target nuclei (strong Coulomb field near the nucleus) the projectiles may experience large-angle scattering and a considerable energy loss (‘nuclear energy loss’). However, beam particles scattered by large angles will leave the bundle of trajectories of the majority of projectile ions and can largely be discriminated against by collimation of the detection system. The energy loss is a statistical process; tables of such energy loss as a function of ion elemental species and beam energy, target material and target thickness were tabulated some four decades ago. Practical problems rather lie in determining the actual thickness (areal density in  $\mu\text{g cm}^{-2}$ ) of a target. Typical carbon foil thicknesses used in beam-foil spectroscopy are on the order of  $10\text{--}20\text{ }\mu\text{g cm}^{-2}$ , about 1/500 of the thickness



of typical writing paper. One of the better techniques to determine the thickness of such foils is a measurement of the energy loss that  $\alpha$  particles of several MeV (from radioactive decays) suffer in traversing such a foil. The relative energy loss can be large (say, 10–20% for the foil thicknesses in the above example) for relatively slow heavy ions (below 100 keV) and will be less significant (a few percent) at high ion energies; however, in order to strip ion beams to high charge states by interaction with the electron gas, target foils need to be thicker to reach the ionization/recombination equilibrium for high-energy ion beams. For a precision lifetime measurement on a foil-excited ion beam one has to determine the energy loss with some precision (know the foil thickness with some precision), or one has to measure the ion velocity after ion–foil interaction, which at high ion energies is rarely practical.

An example: if the total energy loss in a target foil amounts to 2%, the velocity changes by 1%. If the foil thickness in this case is known to 20%, this adds an uncertainty of 0.2% to the time scale of an atomic lifetime measurement that relies on the ion velocity. Such an uncertainty poses some restriction on the ultimate accuracy of an atomic lifetime measurement using foil excitation of fast ion beams, but other problems may be larger. The most accurate beam–foil lifetime measurement (with a lifetime uncertainty of 0.26%) has been achieved on the  $1s3p\ ^1P$  level of neutral He atoms [14]. The fast ion beam ( $\text{He}^+$ ) was sent through a thin foil to pick up an electron into an excited state. Part of the precision of the experiment is owed to a direct measurement of the ion velocity after the interaction with the foil. This was achieved by observing quantum beats, a result of the coherent excitation of  $1s2p\ ^3P$  fine structure levels in the same atomic species. Based on accurately calculated fine structure intervals predicting the beat frequency, the observation of the  $2s\text{--}2p$  triplet transitions concurrently with the decay of principal interest (at a different wavelength) provided reliable clock pulses along with the decay curve and removed the need for a determination of the ion velocity. Fine structure intervals increase with the fourth power of the nuclear charge  $Z$ ; the higher spatial frequency of associated quantum beats in combination with various other technical factors makes it difficult to observe quantum beats in multiply charged ions with sufficient contrast.

Laser spectroscopy, especially collinear laser spectroscopy in which a laser beam co- (or counter-) propagates with a fast atom or an ion beam, is another approach to determine the particle velocity, via the Doppler effect. This will be discussed below. However, the  $Z$  scaling behaviour of atomic energy levels (and their term differences) makes it impractical to use lasers for this purpose for more than a few transitions in atoms or singly charged ions, because in more highly charged ions the transitions to the first excited levels mostly fall into the VUV. If in beam–foil lifetime measurements the exciter foil is replaced by a (dilute) gas target, the areal density of the target is much lower than that of a (solid state) foil, and hence the energy loss is almost negligible. Both the ion beam and the collisionally excited target gas can be exploited for spectroscopy, the latter with very little Doppler broadening and shift, which is beneficial for precision work. However, the excitation zone of any

differentially pumped gas target will be much more spread out along the ion beam, and therefore the time resolution of prospective atomic lifetime measurements is much poorer, along with the much lower signal level.

The dominant error problem in atomic lifetime measurements using beam–foil techniques arises from the very same feature that makes beam–foil spectroscopy so attractive: the excitation takes place at high electron density (about  $10^{24}\text{ cm}^{-3}$  inside a carbon foil), for a time on the order of  $10^{-14}\text{ s}$  (time of flight through a 100 nm thin foil), before reaching good vacuum again (with turbomolecular pumps,  $p \approx 10^{-6}\text{ mbar}$  or particle density  $n \approx 3 \times 10^{10}\text{ cm}^{-3}$ ). The ion beam itself is very dilute; at ion beam currents on the order of microamperes, the typical longitudinal distance between beam ions is larger than the thickness of the exciter foil (notwithstanding the much wider distribution across the multi-mm<sup>2</sup> beam cross section). Inside the exciter foil, the collision frequency is so high that radiative decays of valence electrons play a minor role; any ion moved to an excited state is more likely to be further excited than to decay, and the interplay of multiple excitation, core excitation and recombination results in a new dynamic balance of charge states and excitation. Practically any excited level of any element in any ion charge state can be reached with some probability. Upon leaving the foil, excitation stops and radiative decay and autoionization take over, moderated by transition zone effects near the rear foil surface where a graded electron density and possible surface electric fields may influence the ions; the time of flight through the transition zone is usually estimated on the order of  $10^{-15}\text{ s}$  which would mark a principal limit of time resolution available from beam–foil lifetime measurements. Lifetime measurements would have to wait until the ions have passed through this zone so that excitation has ended and the decay becomes truly exponential, all the while short-lived levels already lose much of their population. A practical limit to such lifetime measurements lies in knowledge of the details of the detection ‘window function’ [15, 16]. A detailed geometric and optical analysis thus gives measurement access to the few-picosecond lifetime range, but the ubiquitous cascades from other short-lived levels have precluded any high-precision lifetime determination in that range so far.

In photon spectra of foil-excited ion beams at positions within micrometre distances from the foil, the spectra are practically continuous, masses of unresolved blends of lines from the decays of extremely short-lived multiply excited levels (see [17]). Superimposed on this dense forest of lines are some resonance transitions which dominate the spectra after a few picoseconds, when the plethora of core-excited states has died out. (Charge state distributions measured by magnetic separation at some distance downstream reflect the situation after that early decay period, not the charge balance reached inside the foil.) The electric dipole transitions appear bright, because they have the highest transition rates (level lifetimes of many picoseconds, in moderately charged ions). When they have died out, the spectrum still shows lines, but only a few, from spin-forbidden decays (intercombination transitions, level lifetimes in the nanosecond range), which can thus be

recognized in such delayed spectra [17]. Higher multipole order decays would be next to show, but their lifetime might be too long to measure by this technique. For our example of  $0.5 \text{ MeV amu}^{-1}$  ions, a 1 m long vacuum chamber would correspond to 100 ns time of flight. The integral over a decay curve corresponds to the initial level population; a decay curve drawn out over 100 ns offers no more integrated signal than another one from an upper level with a 1 ns lifetime, but the signal per ion beam path length interval is much lower and competes with the detector noise.

Researchers have tried to measure longer lifetimes by beam–foil spectroscopy, with decay lengths (ion velocity times level lifetime) approaching 8 m [18–21], and the measurements have suffered (initially unrecognized) massive systematic errors. In this case the largest problem turned out to result from imperfect charge state separation. The desired ion species was  $\text{Ar}^{16+}$ , and the  $1s2s \ ^3S_1$  level M1 decay rate (lifetime predictions near 212 ns) was to be measured. The measured result fell 20% short of expectation. Theoretical arguments [22] later pointed out that  $\text{Ar}^{15+}$  ions with  $1s2s$  inner electrons and a third electron in a very high  $n$  state would radiate at practically the same x-ray energy while featuring a slightly shorter lifetime (because of an additional autoionization decay channel). The presumed measurement on only He-like ions might thus have suffered from a substantial contamination by Li-like ions with a spectator electron. Phenomenologically, this hypothesis was later corroborated by experiment [23], showing that the apparent lifetime depended on how soon after leaving the foil the lifetime measurement started, and that for later times the contamination died out and the apparent lifetime came close to expectation. The lifetime result was still not as precise as originally hoped for, but other types of measurement (ion traps, see below) have taken over for such long atomic lifetimes and have reached much smaller uncertainties since. Irrespective of the actual numbers, the phenomenon of spectator electrons in high-lying levels has become a recurrent theme in the quest for accurate lifetime measurements.

The principal problem for accurate atomic lifetime measurements with the beam–foil technique is the non-selective excitation. If each decay proceeds with an amplitude proportional to the level population and no other interaction, the single exponential of each decay branch would be easily evaluated. However, not all decays proceed directly to the ground state, and thus the populations of excited levels are being replenished by the decays of other levels. This implies that their own decay curves gain additional components that reflect the cascade effect. Curtis [24] has shown how these components preserve the lifetime information of their level of origin, but also how the relative amplitudes of the exponentials combining to a real-world decay curve depend on the differences of the decay rates involved. Depending on the relative level lifetimes and on the data statistics, there can be cases which are easily evaluated by multi-exponential fitting and others that are practically intractable; most are somewhere in between. Programmes have been developed that avoid human interference when trying different numbers of fit components. Often there are several combinations of

amplitudes and time constants that on statistical grounds ( $\chi^2$  value) appear similarly valid and that can be decided upon only by considering the atomic structure situation. If one can measure all cascades that feed a level, the true lifetime of that level can be obtained reliably from a procedure that correlates the cascades with the decay curve of primary interest. This ANDC process (arbitrarily normalized direct cascades [25]) does not require to establish the relative amplitudes of the cascades, but only their time dependence. Hence, other decay branches of the cascade levels can be used, if they are better amenable to measurement. In order to reduce the influence of the role of statistical scatter, the actual decay curves can be replaced by multi-exponential representations that are not required to use physically meaningful individual components [26]. Incidentally, such a recipe works best in several cases where it is needed most, that is for displaced levels in ions with a few electrons in the valence shell.

A representative case is Be-like ions (4 electrons, of which two are in the closed K shell), with the resonance transition  $2s^2 \ ^1S_0 - 2s2p \ ^1P_1^o$ . Early beam–foil lifetime measurements on this prominent line in various Be-like ions returned lifetime values some 40–50% longer than predicted. The reason is a growing-in cascade from the  $2p^2 \ ^1S_0$  level which has a lifetime that is some 20% shorter than that of the primary level. Because of the cascade repopulation with almost the same time constant, the primary level population hardly drops initially, and uneducated multi-exponential fits then return one component that represents two, and with a significantly wrong (unphysical) slope. (Engström has presented a number of illuminating examples of such data [27].) In neutral Be, however, the measured result agreed well with prediction, but it does not do so in the heavier ions: in  $\text{Be}^0$ , the  $2p^2 \ ^1S_0$  level lies above the ionization potential and thus autoionizes—the specific radiative decay cascade is absent. A second, much slower cascade from the  $2p^2 \ ^1D_2$  level, poses no particular fit problem (although it collects like a funnel the cascades from many high- $n$ , high- $\ell$  levels—among them the chain of yrast levels of maximum angular momentum  $\ell$  for a given value of  $n$ —that boosts the line intensity of the resonance line). (The notion of ‘wildly spinning’ yrast levels originates from similar high-spin levels in nuclear physics.)

Because transition probabilities of resonance lines are of fundamental and applied interest, they have been calculated often, and the scatter of the experimental lifetime data seemed worrying. Several attempts were made to critically evaluate the experimental results and to determine a set of recommended data for the Be isoelectronic sequence [28–30] guided by isoelectronic fits of the resonance line strength, and clearly there is such a set of reliable results once the experimenters apply either the ANDC technique or a cascade model based on simplified theoretical assumptions and approximate level populations. Now data on the resonance transition rate in Be-like ions up to  $\text{Kr}^{32+}$  agree with a fit curve (and with theory [31]) to within about 2–3% (see also [12]). However, the individual experimental lifetime data carry larger error bars (5–10%), which the authors estimated because of the evaluational problems. In this case the ANDC technique has reduced the systematic error by at least an order of

magnitude, but the cascade situation nevertheless limits the accuracy of the results much more than the excellent counting statistics might promise. (Recent large-scale calculations of the resonance transition probability in Be-like ions carry theoretical uncertainty estimates on the order of  $10^{-4}$  [31], way beyond what experiment can deliver.) The cascade situation is rather similar for the  $n = 3$  levels of Mg-like ions, but in that case a third major cascade ( $3s3d\ ^1D_2$ ) contributes to the complexity. In both isoelectronic sequences, the spin–orbit interaction opens a decay channel of the  $np^2\ ^1D_2$  level to the  $nsnp\ ^3P^o$  term. The decay channel is easily recognized by its shortening effect on the  $np^2\ ^1D_2$  level (and cascade) lifetime [32], but the lifetime data are of limited accuracy. Even so a systematic comparison with theoretical predictions indicates that theory needs substantial refinement for a proper treatment of this intercombination decay channel.

When employing the ANDC prescription on these decays and cascades, all transitions are of the  $\Delta n = 0$  type with wavelengths in the same range, which are accessible to the same detection equipment. There are also cascades from the higher electronic shells, with wavelengths in a much shorter wavelength range and with level lifetimes that usually are much shorter. In most laboratories there will be neither the spectroscopic equipment to obtain ANDC cascade data on all relevant cascades nor will it often be possible to measure the time constants of fast cascades, and some ambiguity remains even when applying the ANDC scheme to the most prominent decays. As mentioned above, cascade models can help to reduce the uncertainties associated with cascades [33]. A complete cure would require selective excitation, or at least a selective change of population as has been demonstrated by laser irradiation of a foil-excited ion beam [34]. Again, lasers are not powerful enough to influence many levels of multiply charged ions. Moreover, the energy straggling and small-angle scattering of beam ions introduced by the ion–foil interaction are large enough to cause a Doppler broadening that exceeds the bandwidth of otherwise suitable lasers, which then are too weak to have much effect. In order to reduce this problem, a thinner target (gas instead of a foil) or an immaterial target (laser light) is advantageous, but either limits the technique to low ion charge states (see the next section).

### 2.3. Laser excitation of fast atomic and ion beams

One of the problems of high-resolution laser spectroscopy is the Doppler broadening in the interaction of light with atoms or ions: narrowband laser light is in resonance with only a velocity group of particles out of a (possibly thermal) distribution in a discharge, an atomic beam or a vapour cell. Incidentally, the match can be improved by accelerating the ions (adding a large velocity to the velocity component in one direction). From ions of an energy distribution  $\pm\Delta U$  (with  $\Delta U$  on the order of up to a few eV) in the source a beam of particles with energy  $U \pm \Delta U$  is formed (with  $U$  on the order of 100 keV, for example), so that along the ion beam direction the relative energy spread is much reduced. This so-called kinematic compression adds a Doppler shift ( $v/c$  times the cosine of the angle between the particle beam and

the laser beam), but the benefit is that many more particles fall within the laser bandwidth. An additional bonus is that the momentum transfer between light and particles is small, so that one does not need to measure afresh the particle velocity after excitation. In fact, in many cases the laser light frequency in the ion beam rest frame can be brought into resonance with an atomic transition (possibly even using two-photon processes exploiting co- and counterpropagating laser and ion beam), and this match can be used to determine the particle velocity. It is no surprise then that lasers have been used for many experiments on ion beams, and high-precision lifetime measurements are among them. Given the availability of intense tunable lasers in the visible, but much less so in the VUV or EUV, it is also no surprise to find the application of lasers largely limited to neutral and singly ionized species. This restriction may be fading in the course of technical progress with lasers.

The employment of a fast particle beam serves the atomic lifetime measurement in the form of tracking the signal during a spatial displacement of either the excitation zone or the detection zone. (The complementary technique of measuring the decay electronically in the time domain is the subject of the next section.) At a beam energy of typically 100 keV a Na atom travels about  $1\text{ mm ns}^{-1}$ , and the decay curves for typical lifetimes of neutral alkali atoms on the order of 10–30 ns can be tracked over convenient distances on the order of 10 cm. In order to make fast atomic beams, beams of singly charged ions are formed first and then sent through an exchange cell of low-pressure Cs or Rb vapour where a fraction of the ions captures an electron. Most of the capture leads to the ground state; in the capture by singly charged rare gas ions, part of the captured electrons end up in metastable levels (at a considerable excitation energy), so that subsequent laser excitation can start from there.

The original schemes of laser excitation of fast beams used a laser that intersects the atom (ion) beam at some angle. Doppler-tuning into resonance was achieved by changing the angle of intersection (figure 2(c)). This geometry has the advantage of a small interaction zone and the option of an efficient dump for the laser light on the other side of the particle beam, so that stray laser light (of the same wavelength as the subsequently detected fluorescence) could be largely suppressed. With better tunable lasers, intersection at  $90^\circ$  (minimum Doppler shift, geometrical advantages) has become an option [37, 38]. For detection, large-solid angle light collection systems are needed. Early on, optical contraptions like an axicon were employed, collecting light from around the particle beam and guiding it to a few small detectors (for a good signal-to-noise ratio). The detection was segmented, so that slight misalignments of the travelling detector stage in relation to the ion beam trajectory (which go along with a change of solid angle of detection) could be detected and largely corrected for. In more recent designs, the mirrors and prisms have been replaced by optic fibres with entrance apertures arranged on a ring around the particle beam and pointing inwards [35–38]. Ion or atom beams of sufficient particle current cannot be collimated to an arbitrarily fine beam diameter. Within the space determined by the apertures,



however, the ‘illumination’ is not necessarily uniform (and may change over time). This limits the perfection of any mechanical alignment of moving stages and particle beam that can be achieved. This problem is seen as a possible reason why some atomic lifetime measurements quoted to 0.25% [39] did not quite agree with much later measurements as discussed below.

Laser excitation of an ion (or atom) beam can also be achieved in a collinear geometry, with the laser co- or counterpropagating. In order to arrange for localized excitation, the particle beam has a velocity slightly off resonance with the Doppler-shifted (in the rest frame of the fast particles) laser light. In a short section with a longitudinal electric field the ions are accelerated (or decelerated), and excitation occurs only in the particle beam volume where in the particle rest frame the laser light is on resonance. This ‘rapid Doppler switching technique’ [40] allows for a number of variations; for example, the excitation zone may stay fixed and the detector moves in order to record a decay curve, or the detectors are stationary and the excitation zone moves by purely electrical voltage changes to the acceleration zone. Although all these techniques and their variants have at times been touted as tools for high-precision atomic lifetime measurements, only a few laboratories have indeed achieved the goal, and often on the same atomic systems as have been studied by the competition. For example, the Berlin (Andrä) and Lyon (Gaillard) groups studied Ba, and the Berlin and Kaiserslautern (Schmoranzner) groups targeted Li and Na.

When 35 years ago laser spectroscopic techniques yielded precise measurements of the lifetime of the 6p level of Ba II ( $\pm 1\%$ ) [41] and, a few years later, of the 6s6p  $^1P_1$  level of Ba I ( $\pm 0.25\%$ ) [42], there was no theory available to match this precision, and there would not be for several decades. The experimenters therefore turned to lighter atomic systems (Li and Na atoms) [39, 43] for which theory did provide numbers. Theory was found to be off the mark—with the exception of the numerical Coulomb approximation [44], which, however, was considered as being too simplistic to be possibly accurate. The small error bars quoted for the Berlin work apparently discouraged the competition (who had slightly larger error bars) from formal publication [43] for a while, until Carlsson (with slightly larger uncertainties) applied a different technique with a slow atomic beam ([45–48], see the next section). Challenged by the laser-fast-beam data, theory evolved and then began to cast doubt on the full quality of the early measurements. Eventually, refined atomic beam experiments [49, 50], line width measurements on ultracold Na [51] and a very different approach using molecular states that involved large internuclear distances [52–55] superseded the old data and corroborated the recently developed better calculations within the experimental uncertainties of 0.1%. Interestingly, some of the earlier measurements with somewhat more conservative error estimates [43, 45] survived unbeaten, but the high-profile competition with theory had been ignited only by the data that seemed to carry extraordinarily (at the time) small errors.

The same techniques as for the alkali atoms have been applied to various levels in rare gas atoms, benefiting from

metastable levels populated in the electron capture gas or vapour target [56–64].

While the agreement between measurement and theory now is excellent for the resonance transition rates of Li and Na atoms, the calculations for heavy alkali species have been lagging considerably (see the discussion in [65]). For experiment, this is just a technical matter of changing elements. For example, using a diode laser intersecting a 50 keV beam of Cs atoms (after electron capture from Rb) and employing a movable detector system, Tanner and Rafac [66–69] have measured the resonance level lifetime to about 0.25%, while Jin and Church measured  $\text{Ca}^+$  to 0.3% in a collinear arrangement [70]. However, in the earlier papers by Tanner and Rafac it has been discussed that measurements with an uncertainty of 0.1% might be attained, but this goal seems to have remained elusive in their own sequence of experiments.

#### 2.4. Laser-induced fluorescence and electronic timing

The fast-beam techniques described before employ the displacement of the excitation or the detection zone along the beam as a tool in probing a spatial decay curve from which then the temporal decay curve is derived. If the target is stationary (in a cell) or almost stationary (in a slow, thermal atomic beam), the time information has to be gained by fast timing. For lifetimes on the order of a few nanoseconds, the timing intervals have to be smaller than 1 ns and reliable to a small fraction thereof, requiring multi-GHz clock frequencies and matching data processing speeds. This became practical only late in the 20th century. At around the same time, Ti:sapphire short-pulse lasers began to outpace lasers that up to then delivered nanosecond pulses as the shortest. The following examples of atomic lifetime measurements relate to this earlier period and technical capabilities.

Laser spectroscopy and time-resolved laser-induced fluorescence (LIF) are standard techniques in many analytical laboratories. Concerning atomic lifetimes, especially of singly charged rare earth ions of astrophysical and lighting industry interest, the University of Wisconsin (Lawler, Den Hartog [71–73]) runs an eminently productive experimental set-up. A pulsed hollow cathode discharge is the source of a slow atom/ion beam that effuses into a  $p \approx 10^{-4}$  mbar vacuum where it is crossed by a pulsed dye laser beam. The delayed fluorescence light is captured by a photomultiplier tube and the decay curve digitized. In most cases, the laser light provides sufficiently selective excitation. The typical lifetime accuracy is on the order of 5%; this is very useful for various applications, but does not qualify for the present topic of high precision.

Pulsed-laser excitation of Li, Na and Bi atoms in a thermal atomic beam, enabling precision atomic lifetime measurements of radiative transition rates to better than 0.5%, has been demonstrated by Carlsson [45, 48]. As it turned out, these measurements complemented the preceding fast-beam work by a very different technique, but the error estimates were less tight. The results agreed with those obtained at Berlin and Kaiserslautern.

A recent experiment using synchrotron radiation has opened up a new avenue: the energetic photons of a



monochromatized light beam were used to both ionize and excite—in a single step—neutral atoms of Ar, Kr and Xe (in a gas cell at  $10^{-4}$  of atmospheric pressure) rather selectively. For the first excited level in  $\text{Ar}^+$ ,  $3s3p^6\ ^2S_{1/2}$ , for example, a lifetime measurement precision of  $\pm 0.4\%$  was reported, as well as  $0.5\%$  measurements of the corresponding lifetimes in  $\text{Kr}^+$  and  $\text{Xe}^+$  [74]. Theory as quoted in that publication appeared to be struggling with cancellation effects that affect the singly charged rare gases very differently, and the accuracy of the measurement was not yet matched by calculation. A later calculation by Saha and Fritzsche [75] is in good agreement with experiment, but covers only a single charge state of a single element, not an isoelectronic sequence. As with most theoretical treatments, there was no estimate of the reliability of the calculations.

### 3. Spin-forbidden and E1-forbidden decays

Intercombination transitions, that is, transitions which represent a spin change and thus connect different multiplicity term systems of an atom or ion, are enabled by spin-orbit interaction. ‘Automatically’ their transition rates are thus lower than those of fully allowed E1 transitions by some four orders of magnitude; in high- $Z$  ions, the change from LS-coupling to jj-coupling reduces the difference to about two orders of magnitude. Intercombination rates of  $\Delta n \neq 0$  transitions increase roughly as  $Z^{10}$  (at low  $Z$ ), whereas those of  $\Delta n = 0$  transitions increase roughly as  $Z^7$ . Many beam-foil lifetime measurements confirm the theoretically expected trends along the isoelectronic sequences, but none of these experiments have reached high accuracy. This may be a result of the need for high ion currents (for sufficient signal) which has been difficult to produce under conditions for high-precision measurements. Selective population has not been possible, exciter foils change their properties (structure and areal density under ion irradiation) and the light collection efficiency in the EUV (for higher charge state ions) is rather low. In the charge state range most suitable for beam-foil spectroscopy, the levels decaying by intercombination decays have lifetimes in the range of many nanoseconds [76].

In very low charge state ions, however, the lifetimes of levels that predominantly decay by intercombination decay (E1,  $\Delta S = 1$ ) may be in the millisecond range. In the same range are the lifetimes of many ground configuration levels of more complex ions that decay only by E1-forbidden transitions, such as magnetic dipole (M1), electric quadrupole (E2) and so on. (For an overview of isoelectronic trends of E1-forbidden transitions, the reader is reminded of [3, 4].) Ions with such long lifetimes are likely to travel out of the observation zone before their radiative decay takes place. Therefore, it is necessary to confine these ions. A plethora of ion traps has been developed since the 1920s. Again, vacuum technology has played a major role. Only when turbomolecular pumps supplanted diffusion pumps, did an (almost) oil-free vacuum of  $p \approx 10^{-8}$  mbar become available as is essential for storing multiply charged ions so that their many-millisecond lifetimes could be measured. Cryopumps and ion pumps have since improved the vacuum

to the level required for storage rings ( $p \approx 10^{-11}$  mbar and better). The subsequent sections will briefly present how this technical progress has enabled increasingly accurate lifetime measurements on such long-lived levels, and which specific problems have shown up that may presently limit the accuracy of atomic lifetime determinations.

#### 3.1. Ion traps

Atomic lifetime measurements using ion traps have been reviewed repeatedly (see, for example, [77–81]) and the reader will find many examples and results in those reports. Hence, this presentation will illuminate the path to accurate lifetime measurements rather than giving another broad-coverage canvas.

Ion traps (see figure 2(d)) use static electric fields (Kingdon) or magnetic fields (with additional electric voltages (Penning)) or a radiofrequency electromagnetic field (Paul), or combinations thereof, in a variety of geometries and sizes, from flat or cylindrical with a 1 mm typical dimension to storage rings which may feature many kilometres of circumference. If ions are to be stored, the recombination by charge exchange (CX) in collisions with neutral particles of the residual gas has to be minimized. Hence, excellent vacuum is tantamount. Present developments at Stockholm and Heidelberg are of storage rings at cryogenic temperatures that should permit the study of low energy atomic and molecular ions, at which energies the large collision cross sections demand extremely low residual gas density. However, it is unlikely that a perfect vacuum and then infinite storage time will ever be reached. Therefore, it is necessary to determine the loss rate from the stored ion sample. The cleanest such situation would be a single ion in the trap, excited by laser light in a non-perturbing way. As long as the ion is responding, it is still there. Indeed, such experiments are actively done, usually with one laser exciting an ion from the ground state to an excited level from where the ion can radiatively decay to a metastable level. A second laser may be available to probe the population of the metastable level by exciting a fast transition from the metastable level. In an extreme case, the lifetime of a metastable level of  $\text{Yb}^+$  that can decay on its own only by E3 radiation has been determined to be on the order of several years [82].

Single ions offer the prospect of being free of detrimental interactions with the neighbours, and they have marked an important step along the way of precision lifetime measurements on, for example, the  $3d\ ^2D_{3/2,5/2}$  levels of  $\text{Ca}^+$  ions [84]. Since the interrogation uses laser light, it comes as no surprise that the experiments show an influence of the laser power. This particular paper discusses the peculiar scatter of half a dozen recent results that are all at a high level of precision. It seems that data evaluation techniques (maximum likelihood versus least squares fitting) yield systematically different results at the 2% error level of this experiment, that is a range of uncertainties an order of magnitude larger than with the E1 transitions discussed above. The question arises whether all lifetime measurements on E1-forbidden transitions are limited to such a precision—fortunately, the answer is ‘no’,

and most likely the measurements on  $\text{Ca}^+$  and its 1s metastable level lifetimes will also reach a higher accuracy eventually.

Atomic lifetime measurements on multiply charged ions received a boost at Berkeley in the 1970s (Prior). The measurements targeted key atomic systems, were heroic and have not been superseded on the atomic systems then studied, although higher accuracies than the 10% that was typical at the time would be desirable. In the 1990s, sources for relatively slow multiply charged ions became available, so that trapping of ions from such sources has become an option that was pursued at Texas A&M (Church) with a later branch laboratory set-up at U of Nevada Reno and with the original electrostatic trap continuing at CalTech (Chutjian). In these experiments, ions were produced in an electron cyclotron resonance ion source (ECRIS), extracted, charge-separated in a magnet, and a beam of the desired species was sent across the cylindrical space of an electrostatic ion trap (EST) set to ‘no trapping’ mode. While the ions traversed the trap volume, the trap voltages were switched on, and the ions in a section of the ion beam were deflected to stay inside the trap, circulating around the central wire. By plan, the ions were injected in the midplane of the cylindrical contraption, and after the observation period, when the voltage was switched off again, they would be ejected so that at least some of them would reach an ion detector mounted on the midplane outside the trap. This ion signal after various trapping times would yield a measure of the ion storage and loss. However, any divergence of the incoming ion beam gives the ions a sideways velocity component so that they probably fill the trap volume during their many revolutions around the central wire, and rather few ions of unspecified charge state are available for the later ion number analysis. The three laboratories have produced lifetime data mostly on C, O, Ar, Mn and Fe [85–95], but the scatter of the results in comparison to other data suggests that the experimental errors in some cases may have been significantly larger than the one or few percent assumed at the time; none of these lifetime data would qualify as highly accurate.

### 3.2. Heavy-ion storage ring

By the mid-1990s, two other trap designs became viable for atomic lifetime measurements on E1-forbidden transitions, that is, heavy-ion storage rings and electron beam ion traps. A heavy-ion storage ring is an extension of the fast-ion beam technique; since the ions circulate in the storage ring, they pass the same section every few microseconds again and again. Compared to the beam-foil technique with a single pass of ions through the foil and in front of the detection system, the detection system still sees only a small fraction of the decay path of long-lived ions, but for extremely long lifetimes, this fraction is just the length of the observation zone compared to the circumference of the ring, some  $10^{-3}$  in the case of a 5 cm field-of-view on the 55 m circumference TSR heavy-ion storage ring at Heidelberg [96, 97]. The photon brightness of such a ring is so low that no passive spectroscopic observations using a classical spectrometer have been tried yet. Interactions with laser light or with an electron target

are permissible inside the ring, whereas the interaction with heavier particles would cause too much accumulated energy loss to keep the ions stored. However, injection of ion beams that have been excited before entering the ring is possible. In any case, no mechanically moving parts are needed for a lifetime measurement, which is a major advantage in the quest for high accuracy.

Another advantage of the heavy-ion storage ring is the fact that ions of a single isotope, charge state and energy (momentum, velocity) are injected. Consequently, any charge changing reactions change the trajectory of the ion in the magnetic dipole fields of the storage ring, and the ions are lost. A pick-up electrode can detect the change and monitor the ion beam current. At multi-MeV ion beam energies, ions of moderate charge state (and with some electrons left) have storage times on the order of a few seconds to half a minute (bare or singly charged ions can be stored for hours, especially at high energies). Compared to radiative lifetimes sought in the millisecond to second range, the finite storage time constant means a systematic correction that amounts to a few percent for long radiative lifetimes and to a fraction of 1% in the optimum lifetime range near 10 ms. By switching off vacuum pumps in sections of the storage ring, the vacuum can be worsened (all in the pressure range of  $10^{-11}$  mbar) and the systematic correction tested by a Stern–Volmer plot, at pressures some three to four orders of magnitude lower than were available in the early lifetime work with ion traps. Hence what had been one of the largest systematic error problems of earlier work has become a small routine correction now.

However, there is a catch: the ion beam diagnostics of heavy-ion storage rings are built to diagnose the properties of successfully stored ion beams that are circulating for minutes or hours. If the excitation occurs before injection, and the radiative lifetime sought is of the order of a few milliseconds, the question arises whether the diagnostics can deal properly with such short time intervals in which the freshly injected (and stacked) ion beam is still settling down. It seems very likely that the transient fields of the fast-switching deflectors affect the circulating ion cloud. ‘Beam stacking’ is being used to increase the current in the ring by slightly displacing the previously injected ions after their first turn in the ring, so that the beam current in the ring can reach about 30 times the current of the injected beam. Various observations indicate that a fraction of the injected ions is lost in the process, until the circulating ion cloud finds a new equilibrium. Injection over some 30 turns corresponds to about 0.1 ms total, and experience shows strong deviations from stability in the first millisecond after injection, so that observational data for this period have to be discarded. This also puts a short-time limit of, say, 0.3 ms [97] on practical radiative lifetime measurements by this technique at the heavy-ion storage ring.

There usually are beam diagnostics based on the recoil ion produced by beam ions in collision with residual gas atoms. These microchannelplate-based detectors are part of beam profile monitors that indicate the position and width of an ion beam inside the storage ring vessel cross section. These detectors have been enlisted in attempts to measure the presence of beam ions in metastable states, because the

collision cross sections of excited ions are larger than those of the dominant ground-state ion fraction. The effect has clearly been seen, but the technique proved to be not very suitable for precision measurements of highly charged ions, because the detectors are also sensitive to VUV light from the same or other decays. Moreover, the signal is dominated by ground-state ions that pass by the detector over and over again, and the detectors occasionally show considerable nonlinearities that are not understood. In some situations, the signal suggested electric waves caused by ion beam bunches, while in other cases the many-millisecond distortions of the usual signal were interpreted as possibly resulting from some heating of the vessel walls by freshly injected ions that were not stored. In laser-induced fluorescence measurements, slow (second-scale) oscillations have been seen that may relate to periodic changes in ion trajectories. Unfortunately, no way has yet been found to properly diagnose the actual ion beam dynamics in the storage ring on a scale of a few milliseconds. The optical observations (passive observations of visible or UV light emission) suggest rather benign behaviour from at most 2 ms after ion injection into TSR, but that is not sufficient as proof. In spite of such problems with ion beam dynamics that are not fully solved, heavy-ion storage rings are among the top contenders for highly accurate measurements of radiative lifetimes. After giving a few examples of the breadth of applications of the heavy-ion storage ring techniques, I will return to discussing specific results.

The Stockholm heavy-ion storage ring CRYRING has been used to address atomic lifetime measurements of singly charged ions. The ions are injected at relatively low energies on the order of 45 keV. At that energy, further ionization of the beam ions by collisions with the residual gas may be unimportant, but collisional de-excitation of metastable levels as well as collisional excitation from the ground-state matter. In fact, the Stockholm group has measured the longest atomic lifetimes in the field, up to beyond 1 min, by carefully mapping out the various collisional processes. Their detection scheme involves a laser to deplete the remaining population of a metastable level at the end of a given storage time interval and measure the fluorescence signal, thus mapping decay curves point by point over many injection–storage–detection cycles [109]. Laser quenching at early times is used as a tool to empty the reference level and to study the collisional population thereafter. The lifetime results are most valuable especially for astrophysics, but the tedious procedure has been in the way of trying for highly precise lifetime data (in the sense of the present review) with few exceptions so far [98–108].

In contrast to this low-energy ion beam, the ESR storage ring at GSI Darmstadt has employed pulsed-laser pumping of the hyperfine level population in the ground state of hydrogen-like  $^{209}\text{Bi}^{82+}$  ions at a beam energy of 200 MeV  $\text{amu}^{-1}$  ( $\beta = v/c \approx 0.59$ ) [110]. The Doppler shift of the laser light in the rest frame of the ions is so large that roughly 480 nm light in the laboratory rest frame affects the 244 nm transition in the Bi ion. The 0.351(16) ms lifetime of the upper hyperfine level was some 15% shorter than expected at the time. Later results on Pb [111] and again on Bi [112] reflect massive improvements of technique so that an uncertainty of as little as 0.4% was reached.

At the Heidelberg TSR storage ring, dielectronic recombination (DR) has been studied by merging a cold electron beam with a cooled heavy-ion beam. Varying the velocity difference of the two beams, the positions of DR resonances can be mapped by the increase of ions of the next lower charge state in a detector behind the next (magnetic field) bend in the storage ring. The cross section for DR is so small that the process can be seen as an almost noninvasive probe of the level population of the ion's initial excitation state. Following the DR signal over time, the decay curves of the lowest triplet level,  $1s2s\ ^3S_1$ , in He-like ions of C and N (and later B) were measured with the unprecedented accuracy of 0.2% [113]. For ions heavier than N, the radiative lifetime is so short ( $Z^{-10}$  scaling) that the ion beam cannot be cooled quickly enough (by merging with a cold electron beam of the same velocity) before the DR experiment, and then the DR resonances cannot be resolved. The same technique reached only 5% accuracy in Li [115], because of the rather long (50 s) atomic lifetime involved, which was longer than the ion storage time constant. A measurement on Be (using the aforementioned difference of collisional de-excitation cross sections between ground and excited states) reached a 2.5% error [116].

If one relegates the ion excitation to the ion source, or to the gas and foil strippers of the tandem accelerator that serves as the ion injector at TSR, no cooling of the ions is actually required and there is no other interference with the ion beam after storing the stacked ion beam. The ions are left coasting (at TSR, for a minimum period of 200 ms, because of switching frequency limits on the kicker magnet at injection), and a photomultiplier (PMT) views the coasting ion beam through a sapphire window in the ultrahigh vacuum vessel [96]. The first passive observations of this kind used a very low noise solar blind PMT on Be-like ions of C. Initially the light was filtered by a suitable interference filter, but depending on the atomic system and the possible contributions of other levels in the same spectral band, this is not really necessary once certain light-emitting vacuum gauges inside the UHV storage ring vessel are switched off. With a high-current beam such as  $\text{C}^{2+}$  and a PMT with a dark rate lower than 1 cps, the decay curves of the  $2s2p\ ^3P_1^o$  level intercombination decay could be followed for more than three decades, and systematic error studies and counting statistics permitted us to determine the 10 ms level lifetime to about 0.14%. After many earlier calculations (reflecting the astrophysical interest in the case) that had scattered by  $\pm 20\%$  and an ion trap experiment that turned out to be wrong by some five (of their) standard deviations, theory had already reached predictions close to what the experiment then found, but with error estimates near 2%. A very large basis relativistic configuration interaction calculation was eventually done that carried an uncertainty of only 0.5% [117]; however, the calculated result differs from measurement by slightly more than the combined error bars. Conceptually an improved experiment seems feasible, with several PMTs used in parallel in order to boost the signal rate. The best atomic system to study is still the same, because it is easy to provide a high ion beam current, and the 10 ms lifetime seems ideal in the



face of known systematic errors. The same intercombination transition has also been measured in the neighbouring ions of B, N and O, but the steep  $Z$ -scaling ( $Z^{-7}$ ) moves the other lifetimes to less convenient values. The results, though, appear mutually consistent along the isoelectronic sequence (see [12]).

A systematic error that has only partly been explored is the possible influence of the motional Stark effect (fast ions crossing magnetic dipole fields). Measurements at different ion beam energies (see [97]) can elucidate this influence that appears to be small, because the term differences in multiply charged ions with several electrons are much larger than the anticipated Zeeman splittings.

Intercombination transition rates can be measured at TSR only for a few low charge states [96, 97, 118–120]. In a wider range of charge states, levels that have only E1-forbidden decays (M1, E2, etc) are accessible, however. The measurements of such lifetimes in C- and O-like ions have resulted in data [121–124] that clearly deviate from various predictions, although some of the theory data providers had declared their calculations to be reliable. Many of the measurements have error bars on the order of 1%, whereas some calculations of E1-forbidden decay rates scatter—depending on the atomic system—by 20% in some cases and by up to factors of 3 or so in others. For low charge state ions, the tandem accelerator injector serving TSR operates with a gas stripper. If higher charge states are required, a foil stripper in the machine or on the path to the storage ring is needed. Although only a single charge state is selected for injection into the storage ring, some atomic systems showed the presence of more decay components than expected. Since CX can be safely excluded, the extra decay components must result from cascades—just as in the case of foil-excitation in beam–foil spectroscopy discussed above. It turns out that in some atomic systems there are levels of very high total angular momentum above the valence shell, and some of these levels cannot decay by low-multipole order radiation. Thus, some levels of excited configurations feature radiative lifetimes that are of the same order of magnitude as the metastable levels in the ground configurations of, for example, the Al- through S-like ions of iron group elements [125–130]. In spite of very good data statistics (which would be good enough for measurements of a precision of a small fraction of 1%), the close coincidence of the time constants of principal and cascade decays may cause evaluational ambiguity and considerable error in some cases. Only extended data sets along isoelectronic sequences in combination with high-quality calculations will lead to a proper assessment of the atomic physics situation and possibly to smaller evaluational uncertainties.

Moreover, when measuring decay curves of the two decay branches of the  $3s^2 3p^2 \ ^1D_2$  level of the Si-like ion  $Mn^{11+}$ , employing interference filters with central wavelengths of 280 and 370 nm, respectively, and 10 nm band pass, the decay components had slightly different time constants, and in the longer wavelength observation, an additional slow component of not yet identified origin was also apparent [131]. Evidently in the same ion, another transition that involves long-lived levels falls into the wavelength interval that the filter lets

pass—there clearly is a need to investigate spectra with high detection efficiency and sufficient spectral resolution to find out what levels might be involved.

Table 1 has two entries for the aforementioned  $3s^2 3p^2 \ ^1D_2$  level of the Si-like ion  $Mn^{11+}$  (and similarly, two entries could have been listed for the isoelectronic neighbour ion  $Fe^{12+}$ ), one from an experiment using an electron cyclotron resonance ion source and an electrostatic ion trap [89] and the other from the Heidelberg heavy-ion storage ring. Only the former claims an uncertainty of less than 1%, while the two results differ from each other by more than 10%. (The situation in  $Fe^{12+}$  is similar, see [125].) Clearly, not both results can be as accurate as claimed. Both types of experiment are internally consistent along the isoelectronic sequence, but the electrostatic ion trap work ends at Fe, whereas the storage ring experiments extend to Co, Ni and Cu as well, and the latter studies' results are consistent with recent multi-reference Møller–Plesset calculations by Ishikawa and his group at San Juan (Puerto Rico), which mark a new standard in *ab initio* atomic structure calculations of many-electron systems. The electrostatic ion trap work at Reno on other levels and ions has a mixed record when compared with other accurate experiments and with apparently good calculations. This case may serve as a caution against taking published error bars of accurate lifetime data at face value; because of such problems, not all data that have been stated by their authors with an accuracy below 1% have been listed in the table. Where several studies have been performed, only the (probably) most accurate have been listed.

Some of the cascades discussed above pose serious evaluation problems, see further discussion below); in any case, multi-exponential decays are rarely evaluated with high accuracy. Uncertainties of a few percent are still good enough (and important) to benchmark collisional–radiative codes used to interpret astrophysical plasma spectra, but it remains difficult to reach high lifetime measurement accuracy in ions with an open  $3p$ – $3d$  shell.

### 3.3. Electron beam ion trap

Electron beam ion traps (EBIT) [132–134] have been used for atomic spectroscopy for well over 20 years [135–137], and for about a decade and a half for atomic lifetime measurements [81]. An EBIT may be seen as a Penning ion trap based on collinear drift tubes with electric potentials for longitudinal confinement and a strong coaxial magnetic field supporting radial confinement; the EBIT-specific additional element is a tightly compressed electron beam along the axis of the cylindrical arrangement (see figure 2(d)). This electron beam serves to produce by collisions (eventually highly charged) ions from neutral gas or from a cloud of low-charge ions, and it provides a space charge with an attractive radial potential drop. All charge states of all elements are accessible this way [133]. For measuring extremely short atomic lifetimes (femtosecond range), the trapped ion cloud can be cooled (shallow confinement potentials, evaporative cooling) so that the Doppler width amounts to less than the natural line width [138]. This measurement technique has also been applied



**Table 1.** Atomic lifetime measurements on ions that have reached uncertainties of 1% or better. The list may well be incomplete; moreover, several measurements that claim small uncertainties but are likely incorrect have been left out.

| Ion               | Level                                                                      | Lifetime $\tau$                           | Transition type | Light source  | Reference |
|-------------------|----------------------------------------------------------------------------|-------------------------------------------|-----------------|---------------|-----------|
| He sequence       |                                                                            |                                           |                 |               |           |
| B <sup>3+</sup>   | 1s2s <sup>3</sup> S <sub>1</sub>                                           | (149.8 ± 0.45) ms                         | M1              | HSR           | [114]     |
| C <sup>4+</sup>   | 1s2s <sup>3</sup> S <sub>1</sub>                                           | (20.63 ± 0.05) ms                         | M1              | HSR           | [113]     |
|                   |                                                                            | (20.589 ± 0.042) ms                       | M1              | HSR           | [114]     |
| O <sup>6+</sup>   | 1s2s <sup>3</sup> S <sub>1</sub>                                           | (956 ± 5) $\mu$ s                         | M1              | EBIT          | [150]     |
| Ne <sup>8+</sup>  | 1s2s <sup>3</sup> S <sub>1</sub>                                           | (91.7 ± 0.4) $\mu$ s                      | M1              | EBIT          | [151]     |
| S <sup>14+</sup>  | 1s2s <sup>3</sup> S <sub>1</sub>                                           | (703 ± 4) $\mu$ s                         | M1              | EBIT          | [152]     |
| Be sequence       |                                                                            |                                           |                 |               |           |
| B <sup>+</sup>    | 2s2p <sup>3</sup> P <sub>1</sub> <sup>o</sup>                              | (97.65 ± 0.5) ms                          | IC              | HSR           | [97]      |
| C <sup>2+</sup>   | 2s2p <sup>3</sup> P <sub>1</sub> <sup>o</sup>                              | (9.714 ± 0.013) ms                        | IC              | HSR           | [96]      |
| B sequence        |                                                                            |                                           |                 |               |           |
| C <sup>+</sup>    | 2s2p <sup>2</sup> <sup>4</sup> P <sub>J</sub> <sup>o</sup>                 | (7.95 ± 0.07/104.1 ± 0.5/22.05 ± 0.07) ms | IC              | HSR           | [119]     |
| Ar <sup>13+</sup> | 2s <sup>2</sup> 2p <sup>2</sup> P <sub>3/2</sub> <sup>o</sup>              | (9.70 ± 0.15) ms                          | M1              | EBIT          | [145]     |
|                   |                                                                            | (9.5737 ± 0.007) ms                       | M1              | EBIT          | [159]     |
| C sequence        |                                                                            |                                           |                 |               |           |
| N <sup>+</sup>    | 2s2p <sup>3</sup> <sup>5</sup> S <sub>2</sub> <sup>o</sup>                 | (5.88 ± 0.03) ms                          | IC              | HSR           | [118]     |
| Si <sup>8+</sup>  | 2s <sup>2</sup> 2p <sup>2</sup> <sup>1</sup> D <sub>2</sub>                | (38.3 ± 0.3) ms                           | M1              | HSR           | [121]     |
| O sequence        |                                                                            |                                           |                 |               |           |
| Si <sup>6+</sup>  | 2s <sup>2</sup> 2p <sup>4</sup> <sup>1</sup> D <sub>2</sub>                | (63.6 ± 0.7) ms                           | M1              | HSR           | [121]     |
| F sequence        |                                                                            |                                           |                 |               |           |
| Ar <sup>9+</sup>  | 2s <sup>2</sup> 2p <sup>5</sup> <sup>2</sup> P <sub>1/2</sub> <sup>o</sup> | (9.32 ± 0.12) ms                          | M1              | EBIT          | [145]     |
| Al sequence       |                                                                            |                                           |                 |               |           |
| Fe <sup>13+</sup> | 3s <sup>2</sup> 3p <sup>2</sup> P <sub>3/2</sub> <sup>o</sup>              | (16.74 ± 0.12) ms                         | M1              | EBIT          | [157]     |
|                   |                                                                            | (16.726 ± 0.020–0.010) ms                 | M1              | EBIT          | [160]     |
| Si sequence       |                                                                            |                                           |                 |               |           |
| Mn <sup>11+</sup> | 3s <sup>2</sup> 3p <sup>2</sup> <sup>1</sup> D <sub>2</sub>                | (11.16 ± 0.10) ms                         | M1              | EST           | [89]      |
|                   |                                                                            | (13.5 ± 0.2) ms                           |                 | HSR           | [131]     |
| Fe <sup>12+</sup> | 3s <sup>2</sup> 3p <sup>2</sup> <sup>1</sup> D <sub>2</sub>                | (11.05 ± 0.1) ms                          | M1              | HSR           | [125]     |
| Cl sequence       |                                                                            |                                           |                 |               |           |
| Fe <sup>9+</sup>  | 3s <sup>2</sup> 3p <sup>5</sup> <sup>2</sup> P <sub>1/2</sub> <sup>o</sup> | (14.41 ± 0.14)                            | M1              | HSR extrapol. | [127]     |
|                   |                                                                            | (14.2 ± 0.2)                              | M1              | EBIT          | [168]     |
| Co <sup>10+</sup> | 3s <sup>2</sup> 3p <sup>5</sup> <sup>2</sup> P <sub>1/2</sub> <sup>o</sup> | (7.66 ± 0.04) ms                          | M1              | HSR           | [129]     |
| Cu <sup>12+</sup> | 3s <sup>2</sup> 3p <sup>5</sup> <sup>2</sup> P <sub>1/2</sub> <sup>o</sup> | (2.37 ± 0.01) ms                          | M1              | HSR           | [127]     |
| K sequence        |                                                                            |                                           |                 |               |           |
| Ca <sup>+</sup>   | 3p <sup>6</sup> 4p <sup>2</sup> P <sub>1/2</sub>                           | (7.098 ± 0.020) ns                        | E1              | FBL           | [70]      |
| Ca <sup>+</sup>   | 3p <sup>6</sup> 4p <sup>2</sup> P <sub>3/2</sub>                           | (6.924 ± 0.019) ns                        | E1              | FBL           | [70]      |
| Ca <sup>+</sup>   | 3p <sup>6</sup> 3d <sup>2</sup> D <sub>3/2</sub>                           | (1.20 ± 0.01) s                           | E2              | RFT           | [83]      |
| Ca <sup>+</sup>   | 3p <sup>6</sup> 3d <sup>2</sup> D <sub>5/2</sub>                           | (1.168 ± 0.007) s                         | E2              | RFT           | [83]      |
| Rb sequence       |                                                                            |                                           |                 |               |           |
| Sr <sup>+</sup>   | 4d <sup>2</sup> D <sub>3/2</sub>                                           | (435 ± 4) ms                              | E2              | HSR           | [102]     |
| Cs sequence       |                                                                            |                                           |                 |               |           |
| Ba <sup>+</sup>   | 6p <sup>2</sup> P <sub>3/2</sub>                                           | (6.21 ± 0.06) ns                          | E1              | FBL           | [41]      |

Transition type: DR, dielectronic recombination; IC E1, intercombination decay; M1, magnetic dipole; E2, electric quadrupole.

Light source: EBIT, electron beam ion trap; EST, electrostatic ion trap; FBL, fast-ion beam laser; HSR, heavy-ion storage ring; RFT, radio frequency ion trap.

to He-like Fe ions [139]; however, the lifetime result differs by a factor of 2 from established theory. The technique thus has not yet achieved high-precision lifetime data, but

(see figure 1) it works in a niche which no other technique presently has reached. An EBIT can also be used for atomic lifetime measurements with electronic timing. For that, the

electron beam energy is either modulated around the excitation energy of a specific atomic level (needs to be isolated, so only few-electron ions have candidates) [140, 141], or the beam is switched off after some ion breeding and excitation period, and the ion cloud then remains in a Penning ion trap [142], for periods of seconds or even minutes. This magnetic trapping mode for radiative lifetime measurements was first demonstrated on He-like  $N^{5+}$  ions at Livermore [142] and has become the standard technique at EBITs.

The same technique was applied to M1 transitions in the visible range at the NIST (Gaithersburg) EBIT [143, 144]. A small monochromator was employed to isolate the spectral line of interest; this option offers flexibility at the cost of throughput (data statistics). The experiments can serve to illustrate several sources of systematic error. Although the energy necessary to produce, for example, the desired ion  $Ar^{13+}$  is less than 800 eV, the Ar lifetime measurements were done at electron beam energies from 1.5 keV to 8 keV, motivated by the higher electron beam current that can be achieved at the higher energy which then results in a higher signal rate. At the same time, a higher gas injection reservoir pressure promises a higher signal rate, but at the cost of a somewhat poorer UHV vacuum in the EBIT vessel, which then requires a higher electron beam energy to maintain a suitable balance of ionization and recombination (CX with the residual gas). Furthermore, the NIST EBIT results at the time showed considerable scatter of the individual run results, much exceeding the statistical errors of the individual data points. The overall results were interesting as first achievements, but at uncertainties of about 7–8% they do not qualify as precision data.

Subsequent work at the Livermore EBIT has addressed a number of systematic errors in lifetime measurements in the visible (ions of some complexity) [145–149] as well as in the x-ray range (two-electron ions [150–152]). The Livermore work demonstrated how CX can distort decay curves: higher electron beam energies than physically warranted for the production of the proper charge state may yield higher signal rates but can lead to significantly misleading data—confirming Bennett and Kindlmann’s aforementioned earlier findings. It is important to not overionize the stored ion cloud. Insufficiently clean vacuum conditions cause ion loss by CX and thus shorten the lifetime of the level of interest; CX rates need to be measured (which is not always practical for a given charge state ion species), and the apparent decay rates have to be corrected for the effect. Measurements in the x-ray range profit from the energy discrimination that x-ray detectors offer; consequently, x-ray lifetime measurements can be almost background-free. In the visible range, photomultiplier tubes have a considerable dark rate from which the true signal has to be separated. While the actual signal easily exceeds the dark rate and thus an uncertainty on the order of 1% was reached in a number of cases, at a much higher level of statistical significance and measurement precision than in the NIST experiments it was also found that data from seemingly similar runs scattered by much more than expected from their actually excellent data statistics. On purely statistical grounds of counting statistics, some of the Livermore EBIT data were sufficient to support claims of 0.1% precision, but the scatter of the individual

measurements was larger and hinted at systematic errors not yet understood or sufficiently controlled. Among these suspected but unsolved issues were load changes (and thus temperature changes) of the hot electron gun upon switching the electron beam that might change the background light in the machine and might pass through the interference filters of the light collection system.

Moreover, the laboratory was only nominally stabilized in temperature. Testing for systematic error sources, the electron beam current was intentionally set to different values. The gas injection pressure was systematically varied and the trend in the data was accounted for; the results suggested strongly that the NIST EBIT lifetime data (which turned out systematically shorter than fairly reliably predicted) had suffered from poor vacuum conditions. Taking all these effects into account, the x-ray lifetime measurements at the Livermore EBIT reached an uncertainty as small as 0.5% and agree well with the best calculations in the market [153–155], but they cannot distinguish between those calculations, which would require a precision on the order of 0.1%. After Drake’s non-relativistic wavefunctions with a relativistic operator [153] and an added relativistic correction by Lin [154], and the several decades of work by Johnson *et al* culminating in fully relativistic calculations to all orders, the two-electron ions have recently also been treated with the inclusion of QED effects by Andreev *et al* [156]; unfortunately, those authors have given their results only for elements with a nuclear charge  $Z$  in a decimal number pattern that disregards the rather many experimental data available. Accepting for the moment the calculations of two-electrons as a reference, the agreement indicates the validity of the experimental measurement scheme to at least 0.5%. The highest-accuracy visible light range transition lifetime measurement at the Livermore EBIT has been achieved on the M1 transition in the ground configuration of the Al-like ion  $Fe^{13+}$  with an error bar of 0.67% [157].

The next step in the quest for high-accuracy lifetime measurements has been made at the Heidelberg EBIT. With a new machine built based on experience with the Livermore EBIT and with a high degree of automation, new parameter ranges were tested and vast amounts of data collected. For example, the drift tube voltages were set to make a deeper trap (about 1 keV) than used at Livermore, and as a consequence a lower ion loss was found upon switching off or lowering the electron beam energy. Some measurements were done with a residual low-energy electron beam current in the observation intervals, and a role of low-energy electrons trapped in the nooks and crannies of the trap was discussed. Most of the possible sources of systematic error were found to be minor, and overall uncertainties of 0.1% were stated for  $Ar^{13+}$  and  $Fe^{13+}$  ions [158–160], with the dominant uncertainty ascribed to CX reactions. The lifetime data overlap within the error bars with the less precise Livermore EBIT data. 0.1% are an intriguing level of accuracy for fairly complex highly charged ions, and the question arises whether theory is up to the comparison. There were quite a number of calculations for both atomic systems. However, although most of the calculations referred to experimental data for the transition energies (calculations of fine-structure intervals

being notoriously poor), and thus only a line strength value  $S$  near the approximate value  $S = 4/3$  for a simplified treatment (non-relativistic single-configuration limit) of the atomic structure problem was needed, the predictions scattered by about 0.5%. In most of the calculations a QED correction to the M1 transition operator was missing; this correction amounts to about 0.45% of the transition rate. When this correction was included, the agreement between experiment and theory worsened, and it remained unsatisfactory even for the group's own extensive new calculations [158, 159]. The mismatch of experiment and good calculations by a multiple of the stated experimental error might indicate unrecognized systematic errors in the measurements and/or shortcomings in the atomic structure theory, possibly pointing at new physics beyond the standard model. Obviously, confirmation of such high accuracy from a second source is needed.

It would be best to apply a different technique in a control experiment. However, the Heidelberg storage ring TSR has a tandem accelerator (requiring negative ions to start from) as the injector, and thus rare gases (except for He) are not available. An electron cyclotron resonance ion source injector project is no longer pursued at Heidelberg, nor is there any plan to use the Heidelberg EBIT as an injector for TSR. This leaves only other EBITs as contenders for the control experiment. Apart from some points that have been mentioned already (such as electron gun temperature variations, thermal stabilization of the apparatus and laboratory), there are other factors that have to be taken into account in any such experiment aiming at high accuracy. For example, the Heidelberg EBIT delivers a higher photomultiplier signal rate from a presumably larger ion cloud in an electrically deeper and physically larger trap than Livermore's. However, the signal-to-noise ratio is about the same, because Livermore appears to use a quieter PMT model, and that is not even the quietest available, so there is room for improvement. Both groups discuss CX with different findings; better control over CX effects would be desirable. The Heidelberg group discusses the role of low-energy electrons 'hiding' in the trap. Similar effects have not been noted at Livermore, but low-energy electrons may still be present. For example, relating to beam-foil experiments at the time, Nicolaides [161] has pointed out that—especially for highly charged ions—electron capture to levels near the ionization limit should be prominent. Possibly there are enough loosely bound electrons near the positively charged ion cloud in the trap (when the electron beam is switched off) so that a reservoir of cascades may perturb high-accuracy lifetime measurements. Such cascades from particularly long-lived 3d levels have indeed shown up in storage ring measurements of Al- through S-like ions; the worst case recognized so far being that of  $\text{Fe}^{13+}$  ions in which the sole  $3s3p3d\ ^4\text{F}_{9/2}^o$  level has a slightly longer lifetime than the  $3s^23p\ ^2\text{P}_{3/2}^o$  level and feeds it selectively [130]. According to collisional–radiative model calculations, this 'rogue' level is not originally populated so highly, but collects a large fraction of cascades from truly high-lying levels (especially after foil stripping in the injector). Under the much lower density conditions in an EBIT, the effect must be much smaller than the massive 9% effect seen at the storage ring. Collisional–radiative modelling suggests that

it might amount to a 0.3% effect in an EBIT, which would be more than the present error bar of the Heidelberg EBIT experiment. (Such a correction would bring the less precise Livermore EBIT result on  $\text{Fe}^{13+}$  ions into agreement with theory [163] including the aforementioned QED correction.) However, no such long-lived cascade level has been identified for  $\text{Ar}^{13+}$  ions yet. Cascades in general have been claimed to be important in EBIT spectra, too, on the basis of collisional–radiative modelling [162]. Actually measuring those cascades directly will have to address the problem of lines that are smaller than 1% of their stronger companions, which would put them into the noise in a typical graphical display of a spectrum. Of such weak lines one has to establish the intensity and the decay constant, and usually in a different spectral range. For the above example of  $\text{Fe}^{13+}$  ions and the M1 transition in the ground configuration (a visible spectrum line near 441 nm), the slow cascades give rise to several EUV lines (30–45 nm), a spectral range in which no time-resolved spectroscopy has yet been tried at ion traps.

The populations of high-lying levels populated at very low collision energies can be very different from what has been studied for more energetic collisions (beam–foil excitation favouring high- $n$ , high- $l$  levels, high-energy binary encounters favouring low- $l$  levels and very-low energy collisions requiring a different description again); the evidence is seen in EBIT x-ray spectra that mimic x-ray spectra from comets under exposure to the solar wind [164]. With sufficiently high resolution, it may be possible to see an electron population near the ionization limit in an EBIT employing a microcalorimeter [165].

Various EBIT groups (Oxford, Livermore, Heidelberg) have tried to excite trapped highly charged ions by visible-light laser. Apparently the exercise turned out much more difficult than expected [166, 167]. However, the first attempt using EUV radiation at the FLASH facility succeeded in exciting the resonance transitions of Li-like ions of Fe [169]. Since then, several heavier ions have been excited as well, but the present emphasis is on wavelength measurements. It should be possible, however, to measure the time structure of the fluorescence and thus the resonance level lifetime as well, which is in the many-picosecond range. It is too early to make an educated statement on the accuracy that may be achieved.

#### 4. Discussion

The above examples show that lifetime measurements to better than 0.5% accuracy have been done on neutral alkali and rare gas atoms as well as on a number of singly charged ions, on a few cases of (spin-changing) intercombination transitions in low charge state ions, on M1 transitions in He-like ions up to charge state  $q = 14+$  and on a few (dominantly) M1 transitions in few-electron ions. In the latter case, the claims for the exceptionally high accuracy of 0.1% (and disagreement with fully-fledged theory) need to be corroborated. Table 1 recalls the 'better than 1% measurements' of lifetimes of ion levels discussed above. Figure 1 delineates the time ranges in which accurate lifetime measurements have been achieved and how they correlate with the vacuum conditions. The lifetime range

of highly accurate (0.1%) lifetime data so far is rather narrow. Other such maps might be drawn for detector properties in various wavelength ranges.

All in all, both experiment and theory have gone through a long process to reach such a high accuracy. It is not yet possible to turn to an arbitrary atomic system and determine (by experiment or calculation) each level lifetime with satisfactory precision. For example, in Cl-like ions the  $3s^2 3p^5 \ ^2P_{1/2,3/2}^o$  ground configuration is closely related to the  $3s^2 3p \ ^2P_{1/2,3/2}^o$  ground configuration of Al-like ions. Only the latter (the ‘green coronal line’ of  $\text{Fe}^{13+}$ ) has been measured at very high precision [160], under favourable circumstances of, for example, the 530 nm wavelength. The former transition (the ‘red coronal line’ of  $\text{Fe}^{9+}$ ) has about the same transition probability and lifetime, but lies at about 637 nm. This means spectral proximity to the glow of the hot electron gun as well as a much lower detection efficiency of typical photomultipliers. The same experimental group who achieved a measurement with a quoted 0.1% uncertainty in one case consequently has not even reached 1% in the other [168]. The latter level lifetime is known to a better precision (less than 1%) from measurements of isoelectronic ions and an extrapolation to Fe [127, 129]. The wavelength of observation, in fact, plays an important role, because detectors suitable for high accuracy work are not available for all of the wavelength ranges of interest. Solar blind photomultipliers can have a very low dark rate and serve well in the near UV and VUV. In the visible, one manufacturer offers hand-selected photomultiplier tubes for reaching a better signal-to-noise ratio, from the apparently notable scatter of photomultipliers produced following the very same recipe and using the same production line. (Manufacturing ‘quiet’ photomultiplier tubes is considered an art and also depends on the availability of low-radioactivity materials. Another manufacturer was not able to duplicate (by far) the excellent performance of one of their own earlier tubes.) In the x-ray range, individual events can be discriminated by their pulse height, which is very favourable for noise rejection.

Measurements and calculations need to be optimized in each case; for most excitation levels, theory will provide the only practical access, but theoretical approximations and algorithms need to be tested and benchmarked. Reliable results tend to be available only from rather massive calculations and from rather involved experiments. (Interestingly, in the days before cheap computing, a judicious choice of wavefunctions allowed Nussbaumer and Garstang to estimate a number of level lifetimes in amazingly good agreement with later work.) However, if a substantial number of atomic lifetimes dominated by various transition types can be determined to 0.1% accuracy, it might well be possible to judge whether or not atomic theory as we know it is ‘complete’, or whether there are indications of ‘New Physics’ beyond the standard model in this quarter.

Theory generally does not predict lifetimes *per se*, but rather transition probabilities. Only for unbranched decays, can the measured level lifetimes be converted directly into transition rates. Measurements of the branch fractions [170, 171] in combination with lifetime data can then

deliver individual transition rates. The branch fractions often depend sensitively on higher order decay modes and on other atomic structure details. The measurement of branch fractions may require a wide wavelength range calibration of the detection system; known branch fractions can provide detection efficiency data. For example, if one could reliably measure the absolute fluxes of radiation from a given atomic system in certain astrophysical objects and tie in the results with reliable atomic data, one could gain information on absorption by the medium between the emitter and the observer [172]. Some of the spectral lines used in such work originate from weak decay channels that are open only because of configuration interaction and similar higher order effects. Some of the branches that are of interest in astrophysical data interpretation may be too weak to measurably affect a level lifetime, but their proper calculation requires codes that can deal with transition probabilities at a high level of reliability. Other transitions involve several electrons and thus possibly relate to lifetimes that are comparable to the typical time intervals between collisions in a dilute plasma; neither experiment nor theory may presently be able to determine all of these decay rates with notable precision. However, attention to the measuring stick of certain atomic lifetimes should be useful to judge the quality of atomic structure calculations. Only if accurate experimental lifetime data are reproduced by *ab initio* calculations, can the latter be considered as being benchmarked and (in a significant aspect) quality-assured.

## Acknowledgments

ET acknowledges support by the Deutsche Forschungsgemeinschaft (DFG). Some of this work was performed under the auspices of the US Department of Energy by Lawrence Livermore National Laboratory under Contract DE-AC52-07NA27344.

## References

- [1] Kirby K 2009 *16th Int. Conf. on Atomic Processes in Plasmas* Transparency text quoted from memory
- [2] Martin W C and Wiese W L online at <http://sed.nist.gov/Pubs/AtSpec/total.html>
- [3] Marrus R and Mohr P J 1978 *Adv. At. Mol. Phys.* **14** 181
- [4] Curtis L J 1984 *Phys. Scr.* T **8** 77
- [5] Wien W 1919 *Ann. Phys.* **60** 597
- [6] Kay L 1963 *Phys. Lett.* **5** 36
- [7] Bashkin S and Meinel A B 1964 *Astrophys. J.* **139** 413
- [8] Bashkin S 1964 *Nucl. Instrum. Methods* **28** 88
- [9] Bashkin S 1965 *Science* **148** 1047
- [10] Bennett W R and Kindlmann P J 1966 *Phys. Rev.* **149** 38
- [11] Träbert E 1997 *Accelerator-Based Atomic Physics Techniques and Applications* ed S M Shafroth and J C Austin (New York: AIP) p 567
- [12] Träbert E and Curtis L J 2006 *Phys. Scr.* **74** C46
- [13] Träbert E 2008 *Phys. Scr.* **78** 038103
- [14] Astner G, Curtis L J, Liljeby L, Mannervik S and Martinson I 1976 *Z. Phys. A* **279** 1
- [15] Träbert E, Winter H, Heckmann P H and von Buttler H 1976 *Nucl. Instrum. Methods* **135** 353



- [16] Baudinet-Ronnet Y, Garnir H P, Dumont P D and Livingston A E 1976 *Phys. Scr.* **14** 224
- [17] Träbert E *et al* 1993 *Phys. Rev. A* **47** 3805
- [18] Schmieder R W and Marrus R 1970 *Phys. Rev. Lett.* **25** 1245
- [19] Marrus R and Schmieder R W 1970 *Phys. Rev. Lett.* **25** 1689
- [20] Gould H, Marrus R and Schmieder R W 1973 *Phys. Rev. Lett.* **31** 504
- [21] Marrus R and Schmieder R W 1972 *Phys. Rev. A* **5** 1160
- [22] Lin D L and Armstrong L Jr 1977 *Phys. Rev. A* **16** 791
- [23] Bednar J A, Cocke C L, Curnutte B and Randall R 1975 *Phys. Rev. A* **11** 460
- [24] Curtis L J 1968 *Am. J. Phys.* **36** 1123
- [25] Curtis L J, Berry H G and Bromander J 1971 *Phys. Lett. A* **34** 169
- [26] Engström L 1982 *Nucl. Instrum. Methods* **202** 369
- [27] Engström L 1993 *Phys. Scr. T* **47** 49
- [28] Reistad N and Martinson I 1986 *Phys. Rev. A* **34** 2632
- [29] Träbert E 1988 *Z. Phys. D* **9** 143
- [30] Curtis L J 1991 *Phys. Scr.* **43** 137
- [31] Jönsson P, Froese Fischer C and Träbert E 1998 *J. Phys. B: At. Mol. Opt. Phys.* **31** 3497
- [32] Träbert E, Pinnington E H, Kernahan J A, Doerfert J, Granzow J, Heckmann P H and Hutton R 1996 *J. Phys. B: At. Mol. Opt. Phys.* **29** 2647
- [33] Träbert E, Doerfert J, Granzow J, Büttner R, Brauckhoff J, Nicolai M, Schartner K-H, Folkmann F and Mokler P H 1995 *Phys. Lett. A* **202** 91
- [34] Baudinet-Ronnet Y, Garnir H P, Dumont P D and El Himdy A 1989 *Phys. Scr.* **39** 221
- [35] Schmoranzner H and Volz U 1993 *Phys. Scr. T* **47** 42
- [36] Volz U, Majerus M, Liebel H, Schmitt A and Schmoranzner H 1996 *Phys. Rev. Lett.* **76** 2862
- [37] Scholl T J, Holt R A, Masterman D, Rivest R C, Rosner S D and Sharikova A 2002 *Can. J. Phys.* **80** 713
- [38] Scholl T J, Holt R A, Masterman D, Rivest R C, Rosner S D and Sharikova A 2002 *Can. J. Phys.* **80** 1621
- [39] Gaupp A, Kuske P and Andrä H J 1982 *Phys. Rev. A* **26** 3351
- [40] Gaillard M L, Pegg D J, Bingham C R, Carter H K, Mlecodej R C and Cole J D 1982 *Phys. Rev. A* **26** 1975
- [41] Andrä H J, Gaupp A and Wittmann W 1973 *Phys. Rev. Lett.* **31** 501
- [42] Andrä H J 1976 *Beam Foil Spectroscopy* ed I A Sellin and D J Pegg (New York: Plenum) p 835
- [43] Schulze-Hagenest D 1979 *PhD thesis* University of Kaiserslautern (unpublished) cited in [39]
- [44] Lindgård A and Nielsen S E 1977 *At. Data Nucl. Data Tables* **19** 533
- [45] Carlsson J 1988 *Z. Phys. D* **9** 147
- [46] Carlsson J and Sturesson L 1989 *Z. Phys. D* **14** 281
- [47] Carlsson J 1989 *Phys. Scr.* **39** 442
- [48] Carlsson J, Jönsson P, Sturesson L and Froese Fischer C 1992 *Phys. Scr.* **46** 394
- [49] Volz U, Majerus M, Liebel H, Schmitt A and Schmoranzner H 1996 *Phys. Rev. Lett.* **76** 2862
- [50] Volz U and Schmoranzner H 1996 *Phys. Scr. T* **65** 48
- [51] Oates C W, Vogel K R and Hall J L 1996 *Phys. Rev. Lett.* **76** 2866
- [52] McAlexander W I, Abraham E R I, Ritchie N W M, Williams C J, Stoof H T C and Hulet R G 1995 *Phys. Rev. A* **51** R871
- [53] McAlexander W I, Abraham E R I and Hulet R G 1996 *Phys. Rev. A* **54** R5
- [54] Tiemann E, Knöckel H and Richling H 1996 *Z. Phys. D* **37** 323
- [55] Jones K M, Julienne P S, Lett P D, Phillips W D, Tiesinga E and Williams C J 1996 *Europhys. Lett.* **35** 85
- [56] Kandela S A and Schmoranzner H 1981 *Phys. Lett. A* **86** 101
- [57] Hartmetz P and Schmoranzner H 1983 *Phys. Lett. A* **93** 405
- [58] Schmoranzner H, Hartmetz P and Marger D 1986 *J. Phys. B: At. Mol. Phys.* **19** 1023
- [59] Marger D and Schmoranzner H 1990 *Phys. Lett. A* **146** 502
- [60] Marger D and Schmoranzner H 1990 *Phys. Lett. A* **150** 196
- [61] Schmoranzner H, Roth H, Volz U and Marger D 1991 *J. Phys. B: At. Mol. Opt. Phys.* **24** 595
- [62] Jin J and Church D A 1993 *Phys. Rev. A* **47** 132
- [63] Volz U, Marger D, Roth H and Schmoranzner H 1995 *J. Phys. B: At. Mol. Opt. Phys.* **28** 579
- [64] Schmitt A and Schmoranzner H 1999 *Phys. Lett. A* **263** 193
- [65] Volz U and Schmoranzner H 1996 *Phys. Scr. T* **65** 48
- [66] Tanner C E, Livingston A E, Rafac R J, Serpa F G, Kukla K W, Berry H G, Young L and Kurtz C A 1992 *Phys. Rev. Lett.* **69** 2765
- [67] Young L, Hill W T III, Sibener S J, Price S D, Tanner C E, Wieman C E and Leone R S 1994 *Phys. Rev. A* **50** 2174
- [68] Rafac R J 1994 *Phys. Rev. A* **50** R1976
- [69] Rafac R J, Tanner C E, Livingston A E and Berry H G 1999 *Phys. Rev. A* **60** 3648
- [70] Jin J and Church D A 1993 *Phys. Rev. Lett.* **70** 3213
- [71] Lawler J E and Den Hartog E A 2002 *Astrophys. J. Suppl. Ser.* **141** 255
- [72] Den Hartog E A, Lawler J E, Sneden C and Cowan J J 2003 *Astrophys. J. Suppl. Ser.* **148** 543
- [73] Den Hartog E A, Buettner K P and Lawler J E 2009 *J. Phys. B: At. Mol. Opt. Phys.* **42** 085006
- [74] Lauer S, Liebel H, Vollweiler F, Schmoranzner H, Lagutin B M, Demekhin Ph V, Petrov I D and Sukhorukov V L 1999 *J. Phys. B: At. Mol. Opt. Phys.* **32** 2015
- [75] Saha B and Fritzsche S 2005 *J. Phys. B: At. Mol. Opt. Phys.* **38** 1161
- [76] Träbert E, Heckmann P H, Hutton R and Martinson I 1988 *J. Opt. Soc. Am. B* **5** 2173
- [77] Church D A 1993 *Phys. Rep.* **228** 254
- [78] Träbert E 2000 *Phys. Scr.* **61** 257
- [79] Träbert E 2002 *Phys. Scr. T* **100** 88
- [80] Träbert E 2002 *Can. J. Phys.* **80** 1481
- [81] Träbert E 2008 *Can. J. Phys.* **86** 73
- [82] Roberts M, Taylor P, Barwood G P, Gill P, Klein H A and Rowley W R C 1997 *Phys. Rev. Lett.* **78** 1876
- [83] Barton P A, Donald C J S, Lucas D M, Stevens D A, Steane A M and Stacey D N 2000 *Phys. Rev. A* **62** 032503
- [84] Knoop M, Champenois C, Hagel C, Houssin M, Lisowski C, Vedel M and Vedel F 2004 *Eur. Phys. J. D* **29** 163
- [85] Yang L, Church D A, Tu S and Jin J 1994 *Phys. Rev. A* **50** 177
- [86] Moehs D P, Church D A and Phaneuf R A 1998 *Rev. Sci. Instrum.* **69** 1991
- [87] Moehs D P and Church D A 1998 *Phys. Rev. A* **58** 1111
- [88] Church D A, Moehs D P and Bhatti M I 1999 *Int. J. Mass Spectrom.* **192** 149
- [89] Moehs D P and Church D A 1999 *Phys. Rev. A* **59** 1884
- [90] Moehs D P and Church D A 1999 *Astrophys. J.* **516** L111
- [91] Moehs D P, Church D A, Bhatti M I and Perger W F 2000 *Phys. Rev. Lett.* **85** 38
- [92] Moehs D P, Bhatti M I and Church D A 2001 *Phys. Rev. A* **63** 032515
- [93] Smith S J, Chutjian A and Greenwood J B 1999 *Phys. Rev. A* **60** 3569
- [94] Smith S J, Cadez I, Chutjian A and Niimura M 2004 *Astrophys. J.* **602** 1075
- [95] Smith S J, Chutjian A and Lozano J A 2005 *Phys. Rev. A* **72** 062504

- [96] Doerfert J, Träbert E, Wolf A, Schwalm D and Uwira O 1997 *Phys. Rev. Lett.* **78** 4355
- [97] Träbert E, Wolf A, Linkemann J and Tordoir X 1999 *J. Phys. B: At. Mol. Opt. Phys.* **32** 537
- [98] Mannervik S, Broström L, Lidberg J, Norlin L-O and Royen P 1996 *Phys. Rev. Lett.* **76** 3675
- [99] Lidberg J, Al Khalili A, Cowan R D, Norlin L-O, Royen P and Mannervik S 1997 *Phys. Rev. A* **56** 2692
- [100] Mannervik S, Lidberg J, Norlin L-O and Royen P 1997 *Phys. Rev. A* **56** R1075
- [101] Lidberg J, Al Khalili A, Norlin L-O, Royen P, Tordoir X and Mannervik S 1999 *J. Phys. B: At. Mol. Opt. Phys.* **32** 757
- [102] Mannervik S, Lidberg J, Norlin L-O, Royen P, Schmitt A, Shi W and Tordoir X 1999 *Phys. Rev. Lett.* **83** 698
- [103] Rostohar D, Derkach A, Hartman H, Johansson S, Lundberg H, Mannervik S, Norlin L-O, Royen P and Schmitt A 2001 *Phys. Rev. Lett.* **86** 1466
- [104] Rostohar D, Andersson K, Derkach A, Hartman H, Mannervik S, Norlin L-O, Royen P, Schmitt A and Tordoir X 1999 *Phys. Scr.* **64** 237
- [105] Derkach A, Ilyinsky L, Mannervik S, Norlin L-O, Rostohar D, Royen P, Schef P and Biémont E 2002 *Phys. Rev. A* **65** 062508
- [106] Hartman H *et al* 2003 *Astron. Astrophys.* **397** 1143
- [107] Hartman H, Rostohar D, Derkach A, Lundin P, Schef P, Johansson S, Lundberg H, Mannervik S, Norlin L-O and Royen P 2003 *J. Phys. B: At. Mol. Opt. Phys.* **36** L197
- [108] Lundin P, Gurell J, Mannervik S, Royen P, Norlin L-O, Hartman H and Hibbert A 2008 *Phys. Scr.* **78** 015301
- [109] Mannervik S 2003 *Phys. Scr. T* **105** 67
- [110] Klaft I *et al* 1994 *Phys. Rev. Lett.* **73** 2425
- [111] Seelig P *et al* 1998 *Phys. Rev. Lett.* **81** 4824
- [112] Winter H *et al* 1998 *GSI Sci. Rep.* p 87
- [113] Schmidt H T *et al* 1994 *Phys. Rev. Lett.* **72** 1616
- [114] Schmidt H T 1994 *PhD thesis* Aarhus, Denmark
- [115] Saghiri A A *et al* 1999 *Phys. Rev. A* **60** R3350
- [116] Träbert E, Gwinner G, Knystautas E J and Wolf A 2003 *Can. J. Phys.* **81** 941
- [117] Chen M H, Cheng K T and Johnson W R 2001 *Phys. Rev. A* **64** 042507
- [118] Träbert E, Linkemann J, Wolf A, Pinnington E H, Knystautas E J, Curtis A, Bhattacharya N and Berry H G 1998 *Phys. Rev. A* **58** 4449
- [119] Träbert E, Gwinner G, Knystautas E J, Tordoir X and Wolf A 1999 *J. Phys. B: At. Mol. Opt. Phys.* **32** L491
- [120] Träbert E, Knystautas E J, Saathoff G and Wolf A 2005 *J. Phys. B: At. Mol. Opt. Phys.* **38** 2395
- [121] Träbert E, Wolf A, Pinnington E H, Linkemann J, Knystautas E J, Curtis A, Bhattacharya N and Berry H G 1998 *Can. J. Phys.* **76** 899
- [122] Träbert E, Calamai A G, Gillaspay J D, Gwinner G, Tordoir X and Wolf A 2000 *Phys. Rev. A* **62** 022507
- [123] Träbert E, Wolf A, Tordoir X, Pinnington E H, Knystautas E J, Gwinner G, Calamai A G and Brooks R L 2001 *Can. J. Phys.* **79** 145
- [124] Träbert E and Gwinner G 2002 *Phys. Rev.* **65** 014501
- [125] Träbert E, Gwinner G, Wolf A, Knystautas E J, Garnir H-P and Tordoir X 2002 *J. Phys. B: At. Mol. Opt. Phys.* **35** 671
- [126] Träbert E, Calamai A G, Gwinner G, Knystautas E J, Pinnington E H and Wolf A 2003 *J. Phys. B: At. Mol. Opt. Phys.* **36** 1129
- [127] Träbert E, Saathoff G and Wolf A 2004 *Can. J. Phys.* **37** 945
- [128] Träbert E, Saathoff G and Wolf A 2004 *Eur. Phys. J. D* **30** 297
- [129] Träbert E, Reinhardt S, Hoffmann J and Wolf A 2006 *J. Phys. B: At. Mol. Opt. Phys.* **39** 945
- [130] Träbert E, Hoffmann J, Krantz C, Wolf A, Ishikawa Y and Santana J A 2009 *J. Phys. B: At. Mol. Opt. Phys.* **42** 025002
- [131] Träbert E, Hoffmann J, Krantz C and Wolf A 2009 in preparation
- [132] Levine M A, Marrs R E, Henderson J R, Knapp D A and Schneider M B 1988 *Phys. Scr. T* **22** 157
- [133] Knapp D A, Marrs R E, Elliott S R, Magee E W and Zasadzinski R 1993 *Nucl. Instrum. Methods Phys. Res. A* **334** 305
- [134] Marrs R E, Elliott S R and Knapp D A 1994 *Phys. Rev. Lett.* **72** 4082
- [135] Beiersdorfer P 2008 *Can. J. Phys.* **86** 1
- [136] Marrs R E 2008 *Can. J. Phys.* **86** 11
- [137] Beiersdorfer P 2008 *Can. J. Phys.* **86** 19
- [138] Beiersdorfer P, Osterheld A L, Decaux V and Widmann K 1996 *Phys. Rev. Lett.* **77** 5353
- [139] Graf A, Beiersdorfer P, Harris C L, Hwang D Q and Neill P A 2002 *Spectral Line Shapes* CP645 ed C A Back (New York: AIP) p 74
- [140] Wargelin B J, Beiersdorfer P and Kahn S M 1993 *Phys. Rev. Lett.* **71** 2196
- [141] Stefanelli G S, Beiersdorfer P, Decaux V and Widmann K 1995 *Phys. Rev. A* **52** 3651
- [142] Beiersdorfer P, Schweikhard L, Crespo López-Urrutia J and Widmann K 1996 *Rev. Sci. Instrum.* **67** 3818
- [143] Serpa F G, Morgan C A, Meyer E S, Gillaspay J D, Träbert E, Church D A and Takács E 1997 *Phys. Rev. A* **55** 4196
- [144] Serpa F G, Gillaspay J D and Träbert E 1998 *J. Phys. B: At. Mol. Opt. Phys.* **31** 3345
- [145] Träbert E, Beiersdorfer P, Utter S B, Brown G V, Chen H, Harris C L, Neill P A, Savin D W and Smith A J 2000 *Astrophys. J.* **541** 506
- [146] Träbert E, Beiersdorfer P, Brown G V, Chen H, Harris C L, Pinnington E H and Thorn D B 2001 *Phys. Rev. A* **64** 034501
- [147] Träbert E, Beiersdorfer P, Brown G V, Chen H, Thorn D B and Biémont E 2001 *Phys. Rev. A* **64** 042511
- [148] Träbert E, Utter S B and Beiersdorfer P 2000 *Phys. Lett. A* **272** 86
- [149] Träbert E, Beiersdorfer P, Gwinner G, Pinnington E H and Wolf A 2002 *Phys. Rev. A* **66** 052507
- [150] Crespo López-Urrutia J R, Beiersdorfer P, Savin D W and Widmann K 1998 *Phys. Rev. A* **58** 238
- [151] Träbert E, Beiersdorfer P, Brown G V, Smith A J, Utter S B, Gu M F and Savin D W 1999 *Phys. Rev. A* **60** 2034
- [152] Crespo López-Urrutia J R, Beiersdorfer P and Widmann K 2006 *Phys. Rev. A* **74** 012507
- [153] Drake G W F 1971 *Phys. Rev. A* **3** 908
- [154] Lin C D 1975 *PhD thesis* Columbia University, New York
- [155] Johnson W R, Plante D R and Sapirstein J 1995 *Advances of Atomic, Molecular and Optical Physics* vol 35 ed B Bederson and H Walther (San Diego: Academic) p 255
- [156] Andreev O Yu, Labzowsky L N and Plunien G 2009 *Phys. Rev. A* **79** 032515
- [157] Beiersdorfer P, Träbert E and Pinnington E H 2003 *Astrophys. J.* **587** 836
- [158] Lapierre A *et al* 2005 *Phys. Rev. Lett.* **95** 183001
- [159] Lapierre A *et al* 2006 *Phys. Rev. A* **73** 052507
- [160] Brenner G, Crespo López-Urrutia J R, Harman Z, Mokler P H and Ullrich J 2007 *Phys. Rev. A* **75** 032504
- [161] Nicolaides C A 1977 *Phys. Lett. A* **63** 209
- [162] Ralchenko Yu, Tan J N, Gillaspay J D, Pomeroy J M and Silver E 2006 *Phys. Rev. A* **74** 042514
- [163] Vilkas M J and Ishikawa Y 2003 *Phys. Rev. A* **68** 012503
- [164] Beiersdorfer P *et al* 2003 *Science* **300** 1558
- [165] Brown G V and Beiersdorfer P 2006 Private communication
- [166] Hosaka K, Crosby D N, Gaarde Widdowson K, Smith C J, Silver J D, Kinugawa T, Ohtani S and Myers E G 2004 *Phys. Rev. A* **69** 011802

- [167] Mäckel V and Crespo López-Urrutia J R *et al* 2008 in preparation
- [168] Brenner G, Crespo López-Urrutia J R, Bernitt S, Fischer D, Ginzl R, Kubiček K, Mäckel V, Mokler P H, Siman M C and Ullrich J 2009 *Astrophys. J.* **703** 68
- [169] Epp S W *et al* 2007 *Phys. Rev. Lett.* **98** 183001
- [170] Lawler J E, Bergeson S D and Wamsley R C 1993 *Phys. Scr. T* **47** 29
- [171] Curtis L J, Federman S R, Torok K, Brown M, Cheng S, Irving R E and Schectman R M 2007 *Phys. Scr.* **75** C1
- [172] Desai P *et al* 2005 *Astrophys. J.* **625** L59